



Research Article

Mineralogy and geochemistry of peridotites and chromitites in the Jijal Complex ophiolite along the Main Mantle Thrust (MMT or Indus Suture Zone) North Pakistan

Zaheen Ullah ^a, Jian-Wei Li ^{a,b,*}, Paul T. Robinson ^{c,d}, Wei-Wei Wu ^e, Asad Khan ^f, Ngo Xuan Duc ^{a,g}, Munir Mohammed Abdalla Adam ^b

^a State Key Laboratory of Geological Processes and Mineral Resources, China University of Geosciences, Wuhan 4330074, China

^b School of Earth Resources, China University of Geosciences, Wuhan 4330074, China

^c CARMA, Key Laboratory for Continental Tectonics and Dynamics, Institute of Geology, Chinese Academy of Geological Sciences, Beijing 100037, China

^d Helmholtz Centre Potsdam, Telegrafenberg, D-14473 Potsdam, Germany

^e School of Earth Sciences, China University of Geosciences, Wuhan 4330074, China

^f Department of Geology, FATA University, Tribal Subdivision Darra, Kohat 26100, Pakistan

^g Hanoi University of Mining and Geology, Hanoi, Viet Nam

ARTICLE INFO

Article history:

Received 4 September 2019

Received in revised form 14 March 2020

Accepted 29 April 2020

Available online 07 May 2020

Keywords:

Geochemistry
Platinum-Group elements
Podiform Chromitites
Jijal complex
North Pakistan

ABSTRACT

The Jijal Complex, one of the largest Neo-Tethyan ophiolites (ca. 150 km²) in Pakistan, occupies a deep-level section of the Cretaceous Kohistan Arc that was obducted along the Main Mantle Thrust or Indus Suture Zone. Peridotites of the Jijal Complex consist mainly of harzburgite and dunite with numerous podiform chromitites. In this paper, we present new mineral compositions, whole-rock major elements, trace elements, rare earth elements (REEs) and platinum group elements (PGEs) to evaluate the melt evolution and petrogenesis of these rocks. Chromian spinel in the chromitites is fairly uniform in composition with Cr#s ranging from 75 to 81, Mg#s from 59 to 63 and TiO₂ < 0.2 wt%, which suggest crystallization from boninitic magmas. Chromian spinel in the peridotites has relatively lower Cr#s of 71–74, Mg#s of 38–48 and very low TiO₂ contents (averaging 0.09 wt%). The Fe³⁺#s of chromian spinels both in the chromitites and peridotites are very low (maximum 0.02), reflecting crystallization under low oxygen fugacity (*f*O₂). The harzburgites and dunites have low average CaO, Al₂O₃ and REE values and contain Al-poor clinopyroxene and high-Cr spinels. Mantle-normalized trace element patterns of the harzburgite, dunites and chromitites reflect high-degrees of partial melting (25%–30%). The high-Cr chromitites all show similar chondrite-normalized platinum group element patterns characterized by enrichment in Os, Ir, Ru and Rh relative to Pt and Pd. The mineral chemistry, whole-rock compositions and PGE geochemistry indicate that the chromitites in the Jijal Complex were generated from a boninitic parental magma generated under low to high *f*O₂ in a supra-subduction zone environment. The calculated compositions of the parental melts of the Jijal chromitites are consistent with differentiation of arc-related magmas.

© 2020 Elsevier B.V. All rights reserved.

1. Introduction

Ophiolitic peridotites are the result of partial melting and melt-rock reaction, processes that are strongly controlled by fluctuations in temperature, pressure, melt flux and oxygen fugacity (*f*O₂) in the upper mantle (Dilek and Furnes, 2014; Lian et al., 2019; Parkinson and Pearce, 1998; Wu et al., 2017; Zhang et al., 2016). The modal mineralogy, mineral compositions and whole-rocks chemistry of these rocks are therefore important indicators of the physical circumstances and tectonic settings under which the ophiolites formed. Most ophiolite

contains at least some chromite deposits in their upper mantle units. The morphology, compositions, chemistry and isotopic characteristics of these chromitites and various mineral inclusions therein provide significant information about the melt-rock interaction, mantle melting and fluid fluxing in the mantle, and also about composition in the deeper earth (Dilek and Yang, 2018; González-Jiménez et al., 2011).

Chrome spinels both from chromitites and residual mantle peridotites have been used as significant indicators for the tectonic setting of ophiolite formation (Arai et al., 2006; Dick and Bullen, 1984; Kamenetsky et al., 2001). In many ophiolite, high-Cr and high-Al chromitites commonly coexist and are presumed to have formed by reactive interactions between peridotite with different degrees of depletion and melts with different compositions (Dilek and Furnes, 2011; González-Jiménez et al., 2011; Llanes et al., 2015; Uysal et al., 2009).

* Corresponding author at: State Key Laboratory of Geological Processes and Mineral Resources, China University of Geosciences, Wuhan 4330074, China.

E-mail address: jwli@cug.edu.cn (J.-W. Li).

The chromitites of high-Cr are considered to be products of boninitic melts produced in forearc environments, whereas high-Al chromitites are considered to be the product of mid-ocean ridge basalt (MORB)-type melts, formed in back-arc setting or mid-ocean ridge at shallow mantle depths (<30 km) (Arai and Miura, 2016). Studies on high-Al and high-Cr chromitites have revealed that most ophiolite contains texturally and compositionally heterogeneous mantle peridotites and extrusive rocks, with various combinations of MORB, island-arc tholeiite and boninite compositions (Dilek et al., 2008; Dilek and Thy, 1998; Dilek and Yang, 2018; Saccani et al., 2017). Proposed models for such complex ophiolites suggest that all these observed compositions and isotopic heterogeneities are likely to develop in a single, evolving supra-subduction zone (SSZ) environment by a combination of magmatism and melt-rock reaction (Derbyshire et al., 2019; González-Jiménez et al., 2011; Kakar et al., 2012, 2014; Lian et al., 2019; Zhou et al., 2014). These features argue strongly for petrogenesis of ophiolites in supra-subduction environments rather than requiring a range of tectonic settings to explain the origin of different mantle melts and the development of different chromitites compositions. Systematic, field-based studies of ophiolites are required to explain the various geochemical characteristics, mineral compositions and isotope geochemistry of podiform chromitites in the mantle peridotites (Dilek and Robinson, 2008).

In this paper we present new data on the mineralogy, mineral composition, whole-rock geochemistry and platinum group element (PGE) chemistry from the upper mantle peridotites and chromitites of the Cretaceous Jijal Complex along the Main Mantle Thrust (MMT or Indus Suture Zone) in North Pakistan (Fig. 1) and discuss their petrogenesis in a Neo-Tethyan geodynamic framework. The Jijal Complex is situated along the southern margin of the Cretaceous Kohistan Island Arc, where it is separated from Indian plate by the Main Mantle Thrust or Indus Suture Zone (Fig. 1; Arif and Jan, 2006). We selected this body for detailed study because its peridotites provide textural, mineralogical and geochemical evidence for formation in a supra-subduction zone (SSZ) setting. The geochemistry of the Jijal peridotites and chromitites has been studied previously by Arif and Jan (2006) and Jan and Howie (1981), but their data were limited to mineral chemistry and they did not focus on the origin of the parental magmas. Using our new observations and data, we discuss the evolving melt compositions of the Jijal Complex and their role in chromitite genesis in a SSZ tectonic setting.

2. Regional geology and structural architecture of the Jijal Complex ophiolite

Tethyan ophiolites (i.e. Kizildag-Turkey, Semail-Oman, Troodos-Cyprus and Waziristan-Northwest Pakistan, Muslim Bagh-West Pakistan, Dongbo-Western Tibet China etc.) are remnants of lithosphere and oceanic crust, along with some supra-subduction zone assemblages that were originated during closure of the Tethyan Ocean and collision of the Eurasia and Gondwana continents (Mahmood et al., 1995; Dilek et al., 2007; Kakar et al., 2012, 2014; Xiong et al., 2015; Dilek and Furnes, 2019). In northern Pakistan, Kohistan Arc Complex (KAC; Fig. 1a) is the exhumed sandwich section between the Karakoram (Asian) plate to the north and Indian plate to the south, and is separated from these plates by major faults, the Main Mantle Thrust (MMT or Indus Suture Zone) and Main Karakoram Thrust (MKT) (Fig. 1a). The northwestern tectonic contact Indian plate is with southeastern part of Afghan block. Both the Indus Suture Zone and western collisional zone with Afghan block contains numerous mafic-ultramafic (ophiolitic) complexes that originally formed within the Neo-Tethyan Ocean (Khan et al., 2007; Mahmood et al., 1995).

The Jijal Complex lies on the hanging wall of the Main Mantle Thrust, and represents mafic-ultramafic roots of the KAC that formed during the arc building stage (ca. 110–90 Ma) (Schaltegger et al., 2002). This complex consists of a lower ultramafic unit and an upper mafic unit (Burg et al., 1998; Ringuette et al., 1999). The ultramafic unit is further divided

into a peridotite zone, a pyroxenite zone and a garnet-bearing hornblende and pyroxenite zone (Fig. 1b). The peridotite zone consists mainly of harzburgite with lenses or bands of dunite, chromite-bearing dunite (Fig. 2a) and chromitite (Fig. 2b). Websterites with stringers of dunite are widespread and become more abundant in upper section where wehrlites are interlayered with the websterite. The transition between the peridotite zone and the pyroxenite zone is marked by an increase in the pyroxene/olivine ratio, while the enrichment of Cr-rich websterite and wehrlite progressively replaced the dunite proportion. The upper part of the ultramafic unit (Fig. 1b) consists of a thin unit (~700 m) of coarse-grained, garnet-bearing rocks, garnet-poor to garnet-rich (\pm hornblende) pyroxenite and (garnet \pm clinopyroxene) hornblende to (hornblende \pm clinopyroxene) garnetite. Overlying the pyroxenites and hornblendites is a garnet-bearing meta-gabbro (garnet granulite) that constitutes the crustal section of the ophiolite, the base of which is considered to be the petrological-MOHO of the Kohistan Arc (Fig. 1b; Burg et al., 1998). Based on field, textural evidences and geochemical arguments, these garnets in gabbros have been interpreted as cumulates of a magmatic assemblage that can crystallise from relatively hydrous mafic magmas at pressure relevant to the lower crust of arcs (Alonso-Perez et al., 2009). The upper mafic section consists of garnet-bearing, meta-gabbros that underwent high-pressure granulite-facies metamorphism ($P > 1$ GPa, $T = 700 \sim 950$ °C) (Arif and Jan, 2006; Ringuette et al., 1999; Yamamoto and Nakamura, 2000; Yamamoto and Yoshino, 1998). Lenses of hornblende, 10–100 m thick, which are roughly subparallel to paleo-moho, are surrounded in the garnets granulite (Fig. 1b). These hornblende become more plentiful upward, and show more or less progressive variation between pyroxene to garnet-rich (\pm hornblende, plagioclase), hornblende to garnet (\pm clinopyroxene, plagioclase) and garnetite to hornblende (\pm clinopyroxenes), with majority of the pyroxenite near the base of the section (Yamamoto and Yoshino, 1998). The Kamila sequence (≥ 10 km thick) is the southern part of the Kohistan Arc represent the upper crustal level, comprises different sorts of fine-grained and layered amphibolite (i.e. ortho-amphibolites, meta-plutonic and carbonates). It is intensively intruded by the amphibolitized rocks of gabbroic to granitic composition which comprise a varied sequence of basalts some with MORB-type tholeiitic affinities and some with island-arc tholeiitic affinities. These amphibolites may be remnants of an upper mafic sequence (Schaltegger et al. (2002).

3. Mineralogy of the Jijal Complex peridotites and chromitites

In the Jijal Complex, the upper mantle peridotites are mainly composed of coarse-grained harzburgite, dunite and chromitites (Fig. 2a, b). The harzburgite comprises olivine (75–82 vol%) (Fo_{90–91}) and orthopyroxene (11–18 vol%) (En_{87–89}, Fs_{7–8}, Wo_{2–4}), with minor amounts of clinopyroxene (En_{49–50}, Fs₃, Wo_{45–47}) (up to 4 vol%) and chromian spinel (up to 3 vol%) (Fig. 3). It has a protogranular texture expressed by intergrowth of olivine and orthopyroxene (Fig. 4a). Some of the olivine grains exhibit resorbed textures, particularly when they are enclosed by large orthopyroxene grain. In some samples, porphyroclasts of orthopyroxene are present. The orthopyroxene commonly hosts clinopyroxene lamellae (Fig. 4a, b) and may show deformational structures such as elongation and development of kink bands. By using the experimental data of Taylor (1998) and Nimis and Taylor (2000), these structures were formed at temperatures of 849 °C to 1007 °C and the estimated pressure condition over this temperature ranges from 17.31 to 22.64 kbar given in electronic supplement (Table S1). Chromian spinel (0.1–1 mm in diameter) is brown to reddish brown, euhedral to subhedral and, in some cases, rimmed by Cr-rich chlorite (kaemmererite). Some unique features typical of high T-P conditions, such as elongation of orthopyroxene and spinels, mechanical twinning of olivine, exsolution lamellae in the orthopyroxene and other plastic deformation structures in harzburgite, confirm that these rocks originated in mantle (~70 km depth; see Xiong et al., 2019).

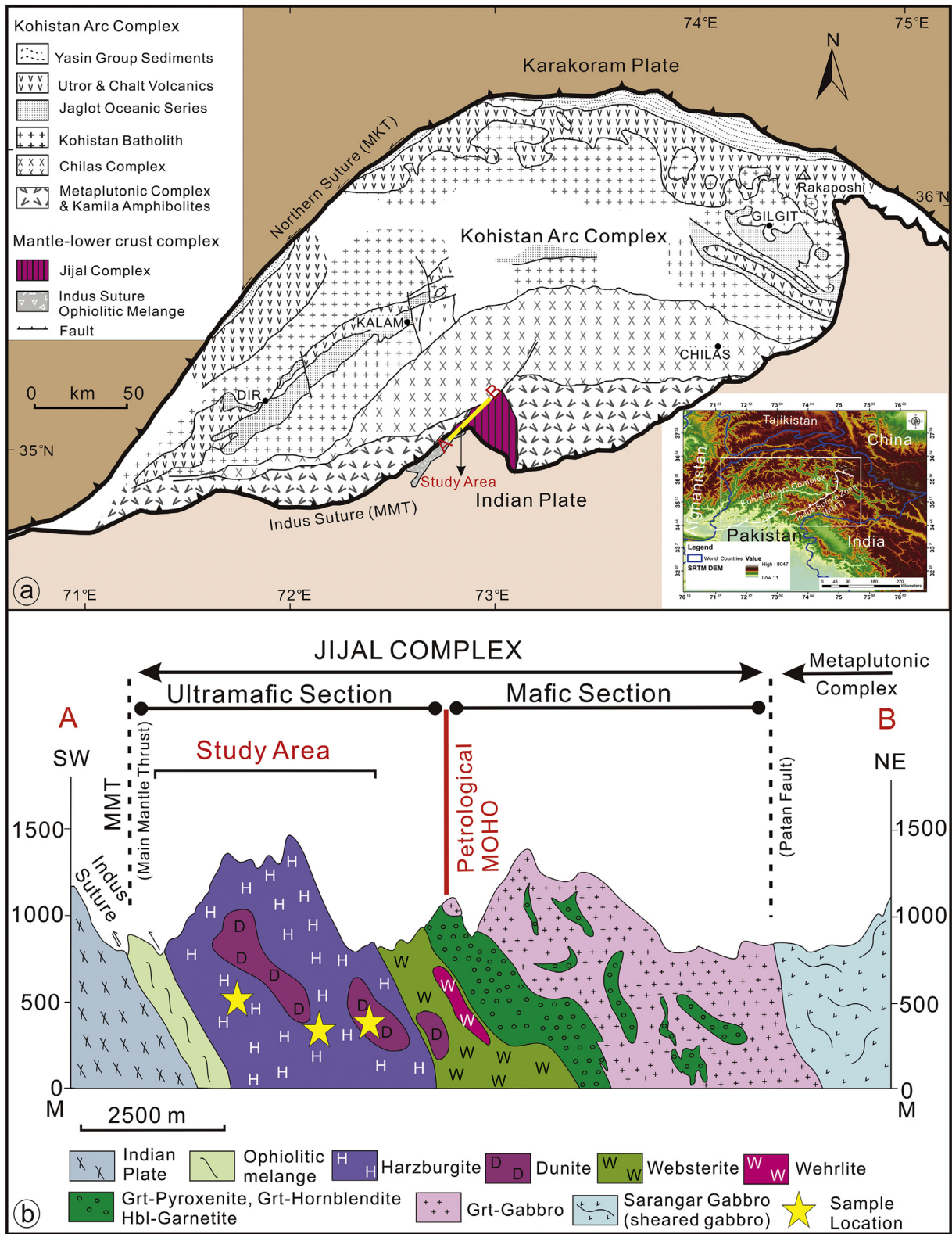


Fig. 1. (a) Simplified geological map of the Kohistan Island Arc Complex (KAC, Northern Pakistan), showing the location of the Jijal Complex (modified after Burg et al. (1998)), the small inset map showing location and topography (light-green is low elevated area and light-white is high elevated area) of Kohistan Arc Complex in north Pakistan (b) Cross-section (A–B) of the Jijal Complex showing that it is a well-defined ophiolite extending from a basal melange through harzburgites enclosing large blocks of dunite to pyroxenites and garnet-bearing gabbro. The mafic portion of the complex has been dated at ca. 85 Ma) (modified after Schaltegger et al. (2002) (see discussion section). (For interpretation of the references to colour in this figure legend, the reader is referred to the web version of this article.)

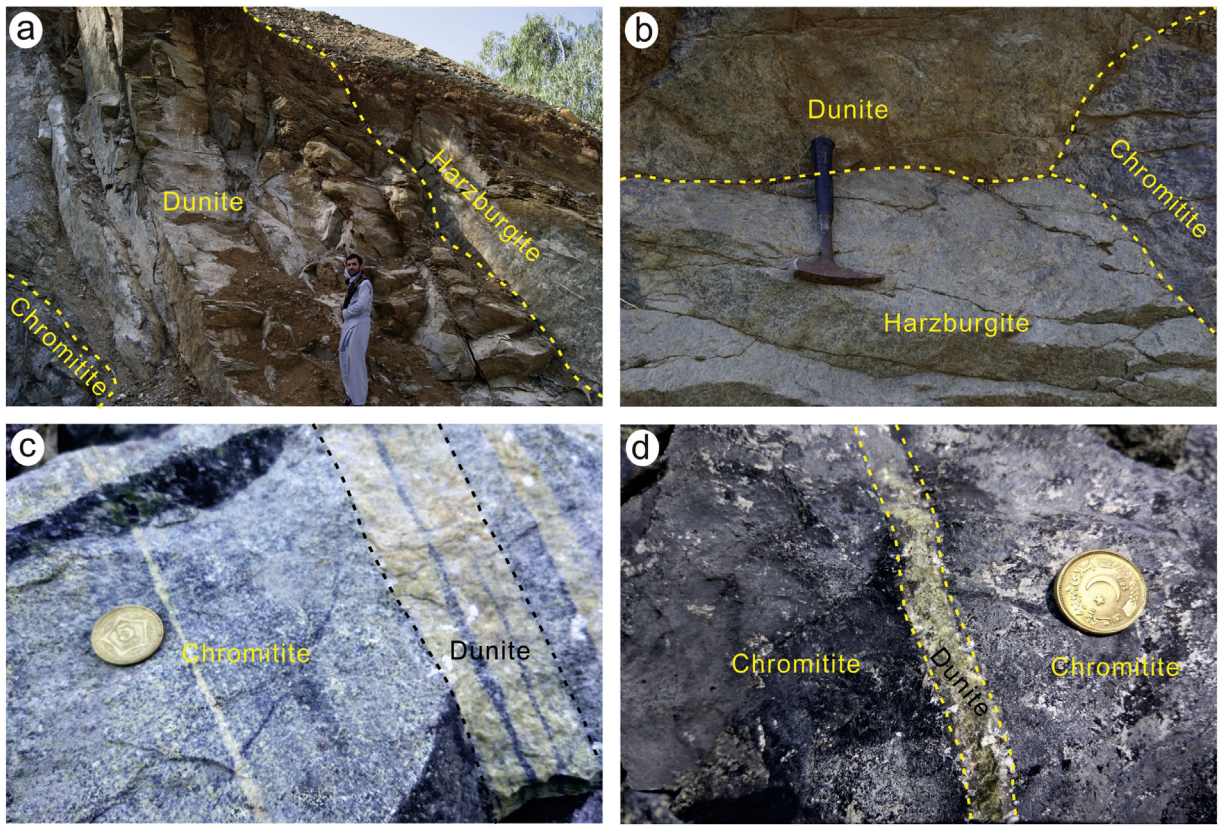


Fig. 2. Field photographs of the Jijal Complex peridotites and chromitites. (a) Dunite occurring as lenses or patches in fresh harzburgite. (b) Chromitite bands in cumulate dunite. (c) Lenses or patches of disseminated chromitite with dunite layers. (d) A dunite band in massive chromitite.

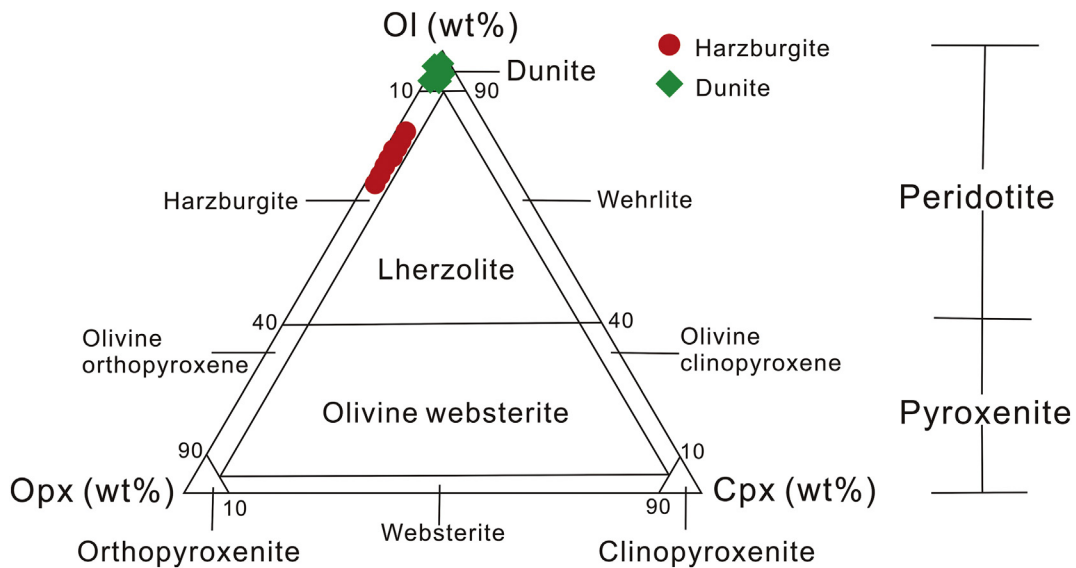


Fig. 3. Modal mineralogy of the Jijal ultramafic rocks. Classification diagram of ultramafic rocks is after Le Maitre et al. (2002). Ol-olivine, Opx-orthopyroxene, Cpx-clinopyroxene.

Dunitic rocks in the study area is dominated by olivine (94–97 vol%) ($Fo_{91.7-92.6}$), with minor orthopyroxene (1–2 vol%), clinopyroxene (1–3 vol%) and chromian spinel (Fig. 3). They are relatively fresh with little serpentinization. These rocks have a granoblastic texture in which olivines grain has curved boundaries, indicating “crystals” recrystallization (Fig. 4b, e). Large olivine grains display deformational kink-band along slip planes, mini-kinking as mechanical twinning, mosaic texture and irregular extinctions band configuration (Fig. 4e). Fine-grained, free-

strain, polygonal olivines crystal probably record static recrystallization in the dunites. The grains of olivine mostly range in size from 0.5 to a few millimetres. Chromian spinels occur as fine (0.1–0.3 mm), subhedral-euhedral, and dark brown grains that commonly host inclusions of olivine (Fig. 4d).

Podiform chromitites occur as massive, semi-massive and disseminated bodies in the Jijal peridotites (Fig. 2c, d). Massive varieties are typically composed of 85–95 vol% chromian spinel, mostly 0.2–0.5

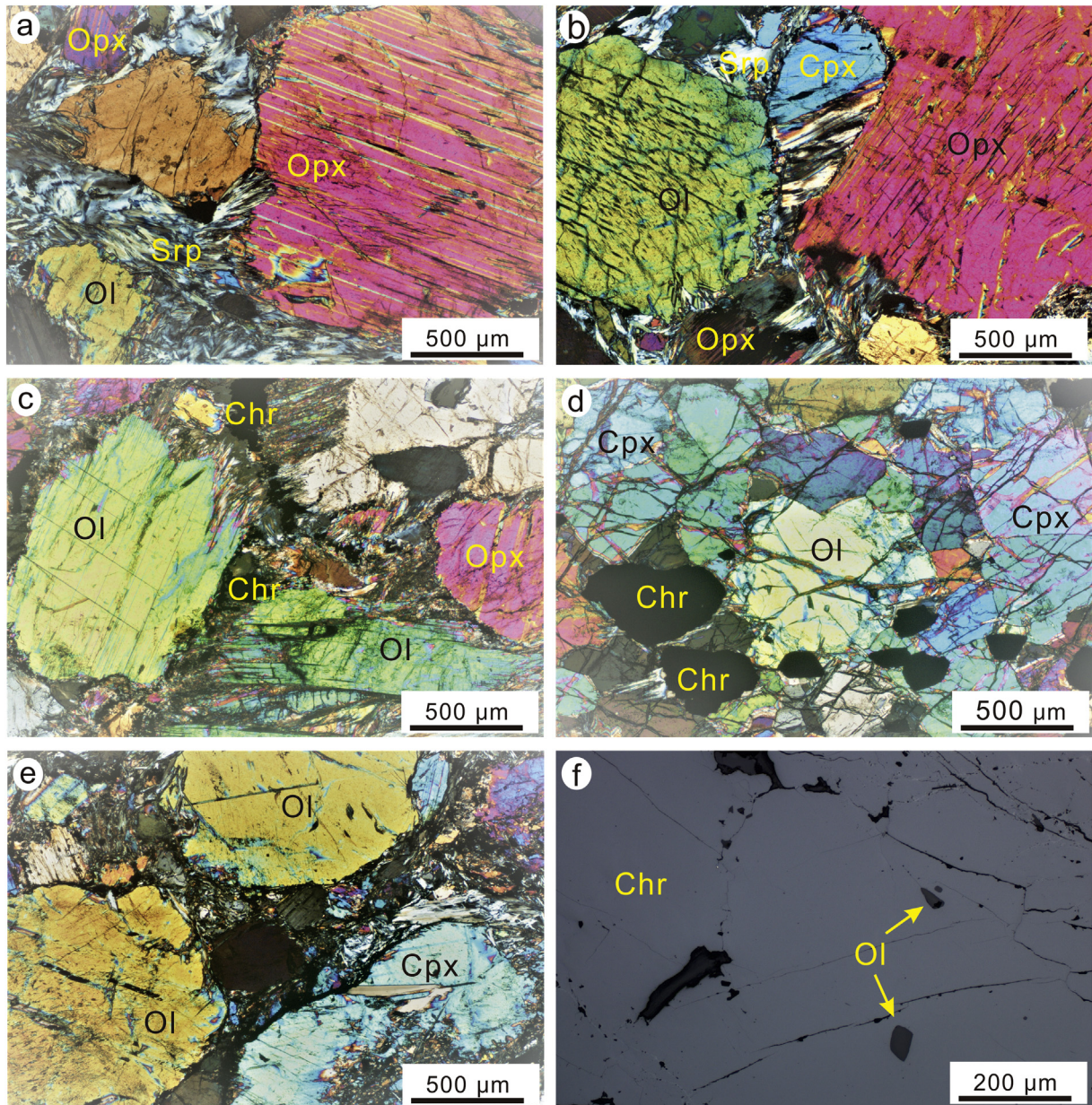


Fig. 4. Photomicrographs of harzburgite, dunite and chromite from the ultramafic section of the Jijal Complex. (a) Harzburgite with coarse-grained orthopyroxene showing clinopyroxene lamellae and serpentine (cross-polarized light); (b, c) Harzburgite with granular texture showing internal deformation and kink banding in partly serpentinized olivine (cross-polarized light); (d) Fine-grained olivine along the contact with fine-grained clinopyroxene and chromite (cross-polarized light) (e) Grain boundary migration in partly serpentinized olivine of dunite (cross-polarized light); (f) Silicate inclusions in chromite. Ol-olivine, Cpx-clinopyroxene, Opx-orthopyroxene, Srp-serpentine, Chr-chromite.

mm across, with sparse relicts of olivine between the spinel grains. Massive chromitites are typically surrounded by dunites, but their shapes and boundaries are usually fractured by numerous faults. They consist of euhedral to subhedral chromian spinels and serpentinized, interstitial relict of olivine crystals. Many grains in these chromitites have abundant silicate inclusions (Fig. 4f). The chromian spinel crystals are commonly fractured with no alteration, and semi-massive chromitites have more relict olivine grains than massive ones.

Disseminated chromitites consist of small (0.2 to 1 mm), euhedral to subhedral grains of chromian spinel with variable proportions of olivine. In some samples the chromian spinels host small, round to elongate grains of olivine (Fig. 4f), orthopyroxene and clinopyroxene, all of which are mostly altered to serpentine, chlorite or clay minerals giving the rocks dark red and/or black colors.

4. Methods and analytical procedures

A total of 50 samples from the mantle units of the Jijal Complex were selected for various analyses, including 10 each of harzburgite, dunite, massive chromitite, semi-massive chromitite and disseminated chromitite (Fig. 2). The sample locations are shown in Fig. 1. The chromian spinel and the associated silicate minerals were analyzed for major elements on polished thin sections by JEOL JXA-8100 electron probe micro analyzer (EPMA) in the State Key Laboratory of Geological Process and Mineral Resources, China University of Geosciences (Wuhan). The analytical parameters of EPMA consisted of accelerating voltage of 15 kV, beam current 20 nA, and counting times of 10–20s. On-line ZAF program was used for the correction of raw data.

Using the method of Qi et al. (2000), trace elements were determined by a jana plasma quant inductively coupled plasma mass

spectrometry (ICP-MS) hosted in Institute of Geochemistry, Chinese Academy of Sciences. Approximately 0.05 g of sample powders were placed in a PTFE, and HF about 0.6 ml and HNO₃ about 3 ml were added and were heated to 185 °C for about 24 h in an electric oven. After cooling, the bombs on a hot plate were heated for the dryness. Five hundred ng of Rh was then added as an internal standard, followed by 4 ml of water and 3 ml of HNO₃. The bomb was sealed again and placed for 5 h in an electric oven to 135 °C to dissolve the residues. The final dilution factor was about 3000 for the ICP-MS measurements after cooling.

For the major elements, the samples preparation method was the same as for the trace elements and with dilution factor of 1000, the elements were measured by ICP-OES (Agilent 720). The traditional gravimetric methods were used for SiO₂ measurement. For LOI determination, about 1 g of sample was heated at 900 °C for about 1 h in a muffle furnace, using the differences in weight before and after heating. The accuracies for the analysis are estimated to be ±5% (relative) for the concentrations of minor oxides between 0.1 wt% and 0.5% and ±2% (relative) for concentrations of major oxides greater than 0.5%. Analytical results and the uncertainties of references material, OU-6 (Slate) and AMH-1 (Andesite) agree well with published values (Potts and Kane, 2007; Thompson et al., 2000). For most elements, the ICP-MS analytical accuracies are estimated to be better than ±5–10% (relative). Detailed analysis processes for PGEs were as described by Xiong et al. (2015).

The peridotite clinopyroxenes trace elements were investigated in-situ on polished thick sections (>80 mm) by LA-ICP-MS at the Sample Solution Laboratory Wuhan, China, with 100 mJ pulse energy and 5 Hz rate of pulse repetition. The ablated materials were flushed in a continuous argon flow into the torch of an ELAN 6100 DRC ICP-MS using an external standard (NIST SRM610) to correct for linear drift.

5. Minerals chemistry

5.1. Olivine

Results of EPMA of olivine from harzburgites, dunites and chromitites are summarized in electronic supplement (Table S2). There are significant differences among the olivine grains from various host rocks and all of the olivine is high in magnesian contents (Fo 90.01–96.87).

In both peridotites and chromitites, olivine occurs as relatively small inclusions in both orthopyroxenes and magnesiochromites. The granular olivine in the harzburgite has Fo values of 90.01–90.85, with NiO contents of 0.26–0.39 wt% and MnO contents of 0.13–0.15 wt%. Both Fo number and NiO contents of the olivine increase toward the dunite lenses and podiform chromitites. Compared to the harzburgite, olivine in the dunite has slightly higher Fo value (91.52–92.06) and NiO contents (0.35–0.44 wt%), but the MnO contents (0.11–0.16 wt%) are similar.

Olivine from the massive, semi-massive and disseminated chromitite bodies of Jijal Complex shows limited compositional variations. Olivine from the massive and semi-massive chromitites, has similar Fo values (94.74–96.87 vs. 94.79–96.86) and NiO contents (0.53–0.69 wt% vs. 0.53–0.68 wt%) Olivine from the disseminated chromitites has Fo of 94.31–96.43 and NiO contents of 0.56–0.67 wt%.

Generally, the magnesian contents of olivines from harzburgite through dunite, disseminated chromitite to semi-massive chromitite and massive chromitite become progressively higher, even though there is considerable overlap between the lithologies (Fig. 5a). Nickel values show a rather steady increase with increasing Fo contents, whereas the MnO contents show a slight decrease among the all lithologies (Fig. 5b).

5.2. Orthopyroxene

Results of EPMA of orthopyroxene from various lithologies are given in electronic supplement (Table S3). Most orthopyroxene in the harzburgites is fresh, but in some highly altered samples it is replaced by bastite and serpentine. It typically forms subhedral porphyroblasts up to 5 mm long but small, anhedral grains are also present in the matrix. In some samples, large orthopyroxene grains display thin exsolution lamellae of clinopyroxene (Fig. 3a–c). Compositional variations of the orthopyroxene depend on the modal mineralogy of peridotites. The enstatite contents of orthopyroxene range from 87.0 to 89.2 in depleted harzburgite, from 89.9 to 91.3 in the dunites, and from 88.4 to 90.4 in the massive chromitites (Table S3). The Al₂O₃ contents of orthopyroxene are also somewhat variable, which are 1.74–2.12 wt% in depleted harzburgites, 0.63–0.89 wt% in dunites, and 0.52–0.71 wt% in the massive chromitites. Chrome contents of the orthopyroxene in all the peridotites are low (0.51–0.72 wt% Cr₂O₃) in harzburgite, 0.11–0.49 wt% in dunite and 0.18–0.45 wt% in massive chromitite (Fig. 5c) The CaO contents of orthopyroxene are 1.39–2.49 wt% in harzburgite, 0.43–1.19 wt% in dunite and 1.74–2.88 wt% in massive chromite (Table S3).

5.3. Clinopyroxene

Harzburgites, dunites, and chromitites contain variable amount of clinopyroxene, which are diopside in composition given in electronic supplement (Table S4). Clinopyroxenes in the harzburgite have the lowest Mg#s (93.1–93.6), which increase to 94.0–95.2 in the dunite with the increasing degree of depletion (Fig. 5e, f). The Al₂O₃ contents of clinopyroxene range from 2.61–2.99 wt% in the depleted harzburgites and 0.62–1.09 wt% in the dunites. These values indicate a negative correlation with the Mg#s (Fig. 5e). Chrome contents (Cr₂O₃) of the clinopyroxene in the peridotites range from 0.69–1.02 wt% in harzburgite and 0.24–0.68 wt% in dunite. Clinopyroxene in different types of chromitite has a range of composition similar to that in the dunites, but has a larger compositional range than that in the harzburgite. The TiO₂ contents of the clinopyroxene correlate negatively with Mg#s; they are usually higher in the harzburgites (0.059–0.096 wt%) than in the dunites (0.01–0.046 wt%). The Na₂O contents of clinopyroxene correlate positively with the Mg#s; the concentration is typically higher in the dunites (0.021–0.075 wt%) than in the depleted harzburgites (0.013–0.052 wt%). Clinopyroxene in the chromitites has the highest concentration of Na₂O.

Clinopyroxenes in the massive chromitites have Mg#s of 95.9–98.2, Al₂O₃ contents of 0.42–0.87 wt% and Cr₂O₃ contents of 0.95–1.83 wt%, whereas those in the semi-massive chromitites have Mg#s of 95.5–96.7 with 0.52–0.98 wt% Al₂O₃ and 1.19–1.74 wt% Cr₂O₃. In disseminated chromitites, the clinopyroxenes have Mg#s of 95.8–96.2 and contains 0.84–0.92 wt% Al₂O₃ and 1.04–1.61 wt% Cr₂O₃ (Table S4; Fig. 5e, f). Detailed microtextural observations of the clinopyroxene grains in the peridotites along with their composition support a residual, rather than metasomatic, origin. In summary, the clinopyroxene closely matches those of typical mantle-derived clinopyroxene from suboceanic peridotites, which show a relative depletion in Na (Fu et al., 2019; Kakar et al., 2012, 2014; Khan et al., 2007).

5.4. Magnesiochromite

Magnesiochromites in the peridotites are residual grains, whereas in chromitites they are primary grains. In serpentinized peridotites the rims of magnesiochromite grains are commonly oxidized to form ferritchromite. Thus, we analyzed only the fresh cores of the grains, and the compositions are given in electronic supplement (Table S5).

Accessory magnesiochromite is very common in the Jijal mantle peridotites, but rarely exceeds 5 modal %. Most of the grains are relatively Cr rich, but some of the harzburgites also contains highly aluminous

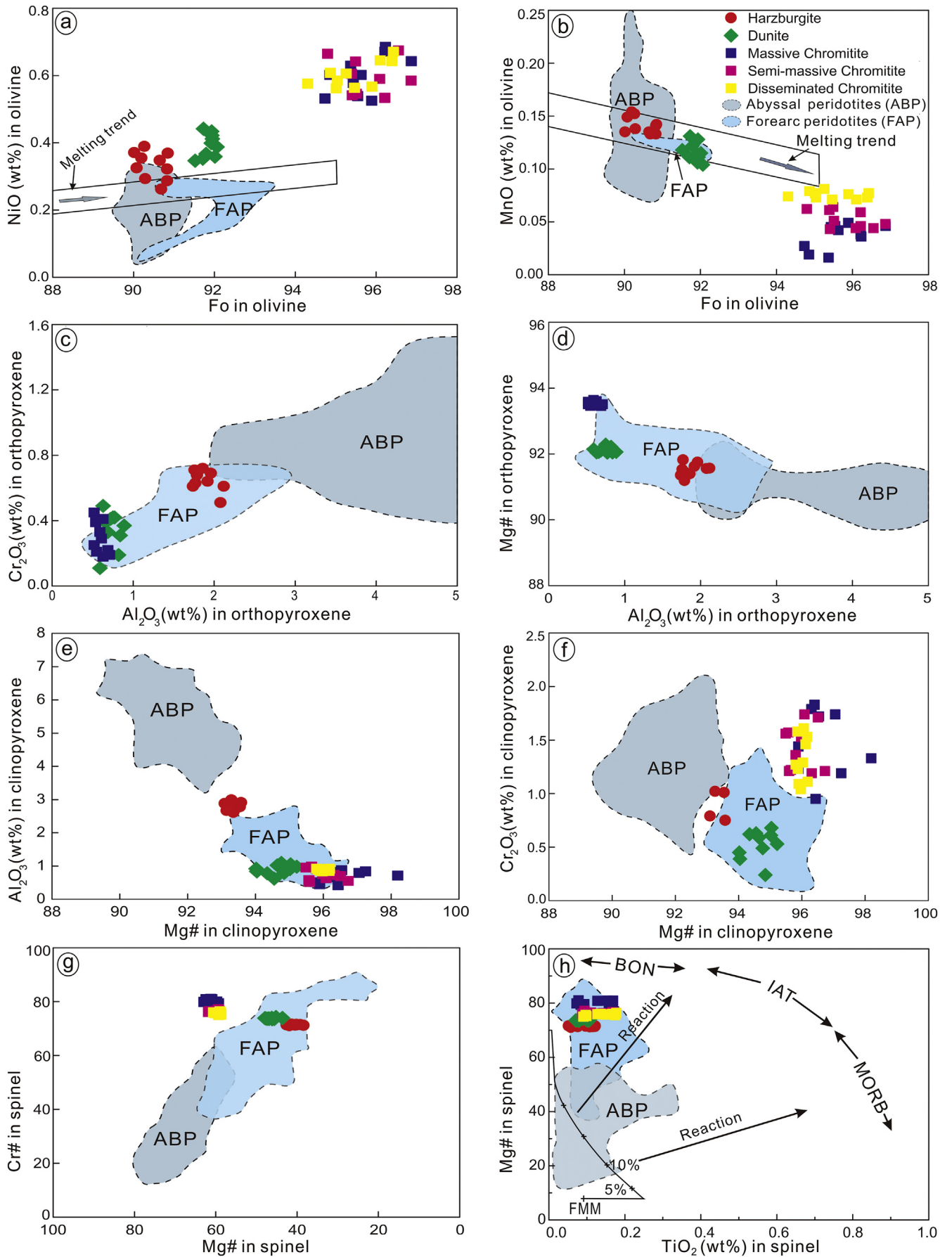


Fig. 5. Compositional variations of olivine, orthopyroxene, clinopyroxene and chromite from the Jijal Complex. ABP (abyssal peridotite) and FAP (forearc peridotite) fields are from Lian et al. (2016) and references therein. The mantle olivine array and partial melting trends are from Saka et al. (2014) and Wu et al. (2017). (a) Olivine (Fo versus NiO); (b) Olivine (Fo versus MnO); (c) Orthopyroxene (Al_2O_3 versus Cr_2O_3); (d) Orthopyroxene (Al_2O_3 versus Mg#); (e) Clinopyroxene (Mg# versus Al_2O_3); (f) Clinopyroxene (Mg# versus Cr_2O_3); (g) Spinel (Cr# versus Mg#); (h) Spinel (TiO_2 versus Cr#).

varieties. The Cr#s ($100 \times \text{Cr}/(\text{Cr} + \text{Al})$) typically correlate with degree of partial melting in the host peridotites and thus provide strong evidence for melt depletion (Dick and Bullen, 1984). Magnesium numbers (Mg#s) also vary with increasing or decreasing the degree of partial melting in mantle peridotites; however, both indices can also be affected by melt-rock reactions. The residual magnesiochromite show a wide-ranging composition, crystal morphology and grain size. Most residual chromite grains are present as large, irregular and commonly amoeboid form. Magnesiochromites in the harzburgites are high-Cr with Cr#s between 71.1 and 71.6 and Mg#s in range of 38.4–42.5; those in the dunites have much higher Cr#s (73.5–74.3) and Mg#s (43.6–47.9). Magnesiochromites included in olivines from dunites are usually euhedral and small-sized crystals, whereas those in the podiform chromitites are mostly large, euhedral-subhedral grains. Magnesiochromites in the massive chromitites have Cr#s of 79.4–80.9, Mg#s of 59.3–62.9, Al_2O_3 contents of 9.12–9.96 wt%, and TiO_2 contents of 0.073–0.169 wt%. In semi-massive chromitites, Cr#s are between 76.1 and 77.2, Mg#s range from 59.1–61.8, Al_2O_3 contents range from 11.17–11.87 wt%, and TiO_2 contents are between 0.088 and 0.175 wt%. In disseminated chromitites, Cr#s are between 75.0 and 76.3, Mg#s range from 58.7–60.5, Al_2O_3 contents are between 11.56 and 12.35 wt%, and TiO_2 contents range from 0.091–0.178 wt% (Table S5; Fig. 5g, h).

6. Whole-rock geochemistry

6.1. Major elements

Geochemical data of whole-rock samples are given in electronic supplement (Table S6). All the analyzed harzburgite and dunite samples are variably altered, as evidenced by the loss-on-ignition values (4.11–11.26 wt%). However, most of the samples preserve their primary mineralogical and textural characteristics, allowing us to examine their petrogenesis and geochemical history. In general, the dunites are less altered than the harzburgites (Table S6), and most appear to have undergone variable degrees of late-stage refertilization (see below). The low contents of CaO (0.06–0.67 wt%) are consistent with the paucity of clinopyroxenes in all the peridotites. The samples are Mg-rich (45.91–50.21 wt%), Al-poor (0.22–0.55), and extremely Na poor ($\text{Na}_2\text{O} < 0.05$ wt%).

In the diagrams of MgO/SiO_2 versus $\text{Al}_2\text{O}_3/\text{SiO}_2$ (Fig. 6), peridotites bulk compositions show a depletion trend slightly below, but parallel to, the terrestrial mantle array (Hart and Zindler, 1986; Wu et al., 2017). In serpentinized peridotites, this depletion may reflect addition of SiO_2 or loss of magnesium. There is a significant decrease in $\text{Al}_2\text{O}_3/\text{SiO}_2$ ratios, but a slight increase in MgO/SiO_2 ratios in orthopyroxene and clinopyroxene during partial melting. As the melting proceeded, it led to consumption of pyroxene, especially clinopyroxene, causing an increase in the modal contents of olivine and in the MgO/SiO_2 ratios. As the degrees of partial melting increased, the bulk MgO/SiO_2 ratios also increased. However, partial melting may not be the only reason for that all the analyzed harzburgites have slightly lower MgO/SiO_2 values than the terrestrial mantle array (Fig. 6), suggesting some Mg loss due to alteration (Niu, 2004; Snow and Dick, 1995). Alteration may also have been responsible for the low concentrations of major and trace elements expected for a given degree of melting. However, the dunite samples have relatively high MgO contents. The forearc and abyssal peridotite fields are shown in Fig. 6 for comparison with our samples. All our analyzed harzburgites and dunites plot in the forearc peridotite field (Fig. 6) characterized by high MgO/SiO_2 values, suggesting high-MgO parental magmas and/or late-stage melt-rock reaction.

The dunites and harzburgites show considerable overlap in their major oxide compositions, ranging from 40.3 to 45.0 wt% in SiO_2 . Both show relatively linear decreases in CaO, Al_2O_3 and SiO_2 with increasing MgO contents (Fig. 7a–c). Total iron as FeO^* shows no systematic changes with MgO contents (Fig. 7d), but some samples plot slightly below the forearc field. Both the harzburgite and dunite samples are

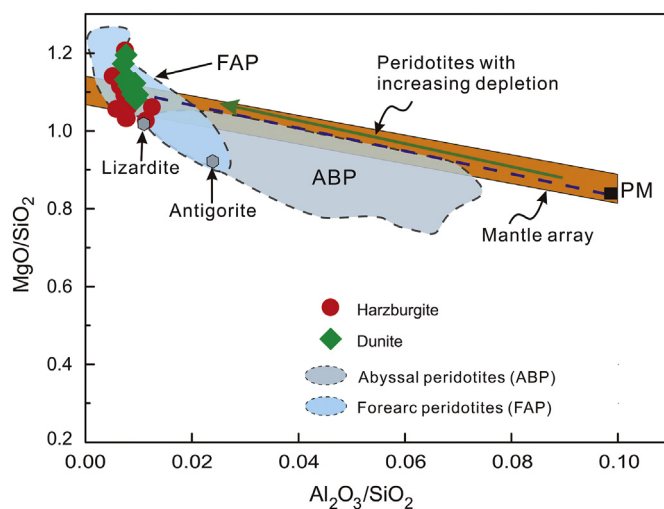


Fig. 6. Whole-rock (WR) MgO and Al_2O_3 contents of the Jijal Complex harzburgites and dunites normalized to SiO_2 . Peridotite depletion trend is from Snow and Dick (1995). Primitive mantle (PM) values are from McDonough and Sun (1995). The data for abyssal peridotites (ABP) are from Niu et al. (1997), and for forearc peridotites (FAP) from Parkinson and Pearce (1998) and Lian et al. (2016). All analyzed harzburgite and dunite samples plot within the forearc peridotite field.

comparable to suprasubduction zone (SSZ) or forearc-type peridotites, but are more depleted than abyssal or Mid Ocean Ridge (MOR-type mantle).

6.2. Trace elements

The total REE inventory of the Jijal peridotites is low, ranging from 0.13 and 0.62 ppm given in electronic supplement (Table S6). The REE concentrations in the harzburgites are higher than in the dunites (0.29–0.62 ppm versus 0.13–0.22 ppm). All the other elements correlate well with MgO contents, except for Ce, La, Nb and Ta (Niu et al., 1997; Parkinson and Pearce, 1998). Co correlates positively with MgO contents because of its compatible nature during partial melting, whereas the other elements are incompatible for olivines. All of the rare earth elements (except for Ce and La) correlate negatively with MgO values (Fig. 8). The chalcophile elements Cu and S have similar behaviour to Al and Ca during partial melting (Luguet et al., 2003); thus, the concentrations of Cu of the samples decrease with increasing degrees of melting (Table S6). In Fig. 8, the Jijal peridotites are compared with those of suprasubduction zone and abyssal environments, which shows that both the major and trace element characteristics of the dunite and harzburgite are comparable to forearc or SSZ varieties. The mantle peridotites in Jijal complex have ΣREE contents well below primitive mantle values (Fig. 9a, b), showing significant depletion, higher degrees of partial melting (Miller et al., 2003; Xu et al., 2011). All the analyzed samples display similar depleted chondrite-normalized patterns (Fig. 9a). The harzburgites display relative enrichment in both light REEs and heavy REEs and depletion in the middle REEs (Fig. 9a). These configurations suggest weak LREE enrichment of previously depleted peridotites, and are consistent with the patterns displayed by most forearc peridotites. The dunite samples show stronger depletion than the harzburgites but still plot in the field of forearc peridotites (Fig. 9a; Parkinson and Pearce, 1998; Pearce et al., 2000).

6.3. Platinum group elements

The platinum group element concentrations of the chromitite, dunite and harzburgite samples are shown in electronic supplement (Table S7). The PGE abundances are low in all analyzed samples, averaging in chromitite 136 ppb, in harzburgite 38.5 ppb and in dunite 29.3

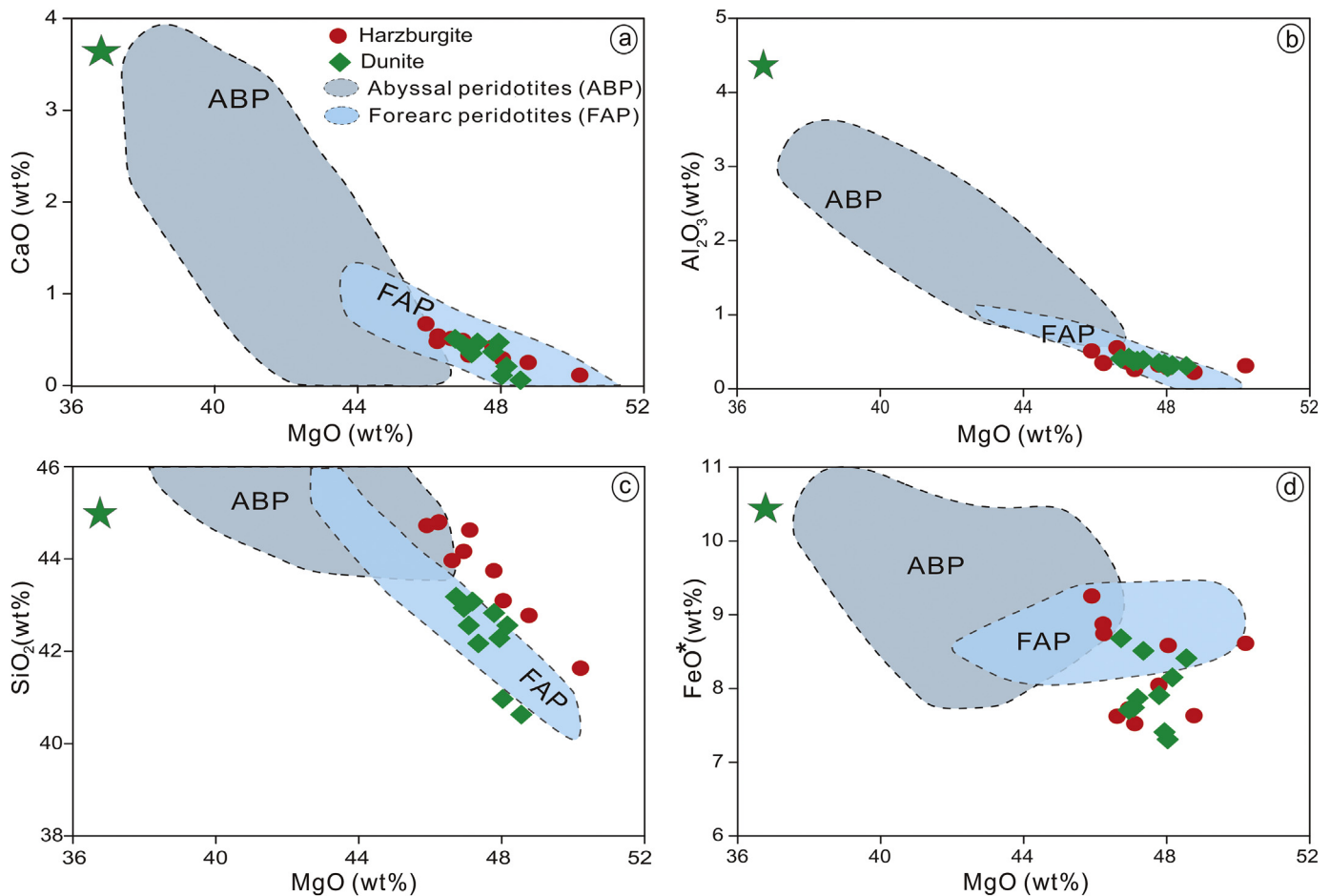


Fig. 7. Harker diagrams showing whole-rock compositional ranges of major oxides in peridotite samples from the Jijal Complex. Compositions are recalculated on a volatile-free basis. The primitive mantle fields are from [Palme and O'Neill \(2003\)](#). Abyssal and forearc peridotite fields are from [Niu et al. \(1997\)](#) and [Parkinson and Pearce \(1998\)](#).

ppb. In the podiform chromitites the total PGE concentrations are within the range of values mainly reported for the chromitite of ophiolites (<300 ppb; [El Ghorfi et al., 2008](#)). The values of Pd/Ir, Ru/Pt and IPGE/PPGE (IPGE = Iridium Group (Os, Ir, Ru), PPGE = Palladium Group (Rh, Pt, Pd)) are 0.033, 46.5, and 11.5 for Cr-rich chromitites, 2.02, 0.81, and 0.89 for harzburgite, and 1.17, 0.89 and 1.17 for the dunite. The Jijal Complex harzburgite samples are PGE enriched compared to the primitive mantle ([Fig. 10](#); [McDonough and Sun, 1995](#)), and depleted relative to their abundances in the chromitites. In the dunite samples the PGE concentrations are slightly higher than those of primitive mantle ([Fig. 10](#); [McDonough and Sun, 1995](#)). The analyzed chromitite samples are typically ~5 times enriched in PGE with respect to their host peridotites, and enriched in IPGE relative to PPGE ([Fig. 10](#)).

7. In-situ trace elements of Clinopyroxene

Selected REE and trace element compositions of clinopyroxene from the Jijal peridotites are given in electronic supplement (Table S8). Clinopyroxenes from the harzburgites have convex, arc-like, chondrite-normalized patterns showing marked depletion in light REE elements ([Fig. 9c](#)), which are similar to those in abyssal peridotites ([Johnson et al., 1990](#)). In contrast, clinopyroxenes in the dunites show notable enrichment in fluid-mobile elements (e.g., U, Pb) with Y and have concave U-shaped or 'spoon-shaped' patterns typical of samples that have undergone melt or fluid impregnation ([Fig. 9d](#)). The clinopyroxene grains in the harzburgites and dunites have extremely low concentrations of highly incompatible lithophile elements as

shown in the primitive-mantle normalized trace element spider diagram ([Fig. 9d](#)).

8. Discussion

8.1. Partial melting of the Jijal complex Peridotites

Modal mineralogy, mineral compositions, and whole-rock geochemical characteristics can be used to assess the degree of partial melting of upper mantle peridotites in ophiolites. The clinopyroxene contents of ophiolitic peridotites reveal only the degree of depletion. Clinopyroxene under the pressure of 2–15 kbar becomes exhausted after 20–26% of anhydrous melting of pyrolitic mantle material ([Gaetani and Grove, 1998](#)). Because of H₂O contribution, the equilibrium between olivine and melt remains unchanged ([Glenn and Timothy, 1998](#)); the olivine Fo composition is a good indicator of the total partial melting temperature. Based on these characteristics, we conclude that the different peridotite types in the Jijal Complex, which comprise variable amounts of clinopyroxenes and olivines with high Fo values (90.02–96.87), underwent different degrees of partial melting.

Many workers have concluded that Al-contents of spinel and pyroxene are sensitive to degrees of partial melting in mantle rocks and that both decrease with increasing depletion of the residue ([Wu et al., 2017](#); [Zhou et al., 2005](#)). The Al₂O₃ of clinopyroxene in the Jijal peridotites correlates negatively with the Cr# values of spinel in which they occur. In the harzburgite, clinopyroxene with low Al₂O₃ contents are in equilibrium with spinel grains with high Cr# values ([Fig. 11a](#)). The

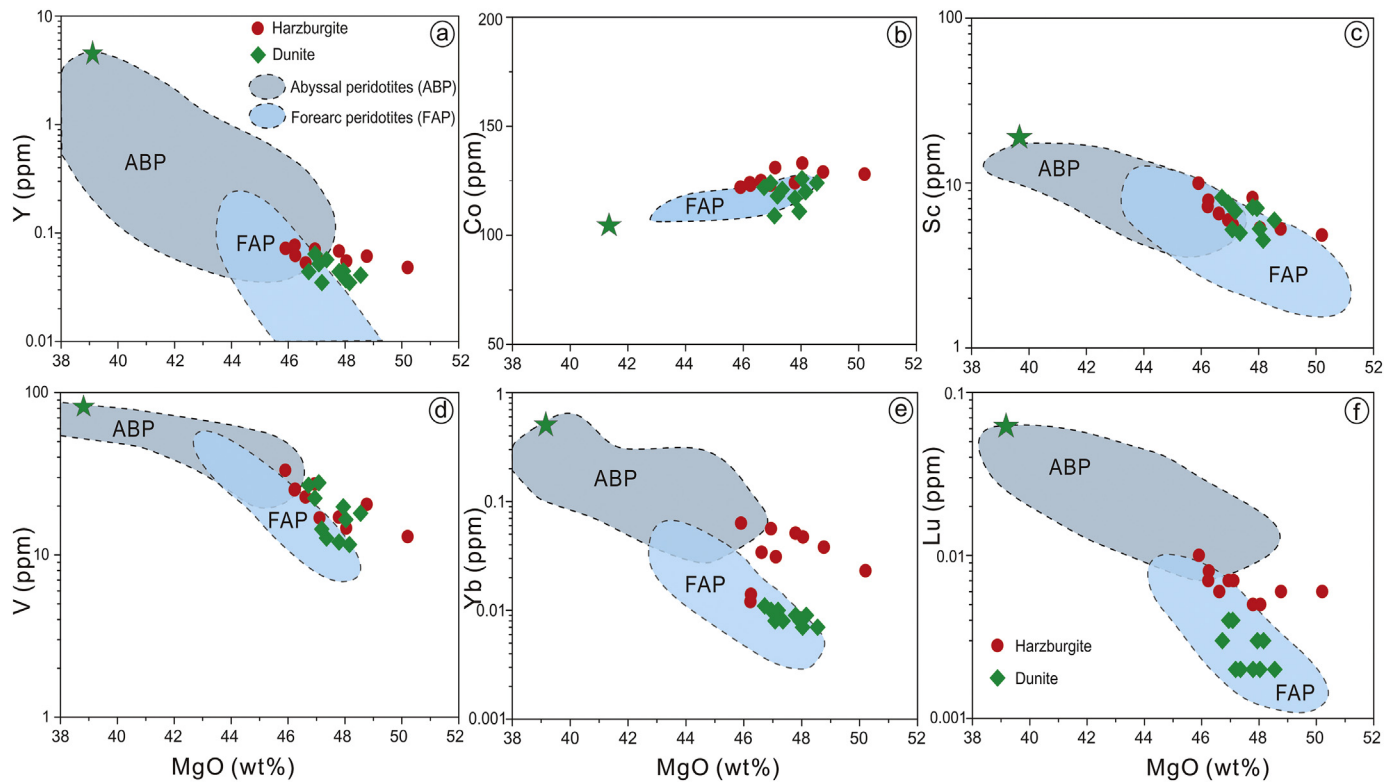


Fig. 8. Variation diagrams of MgO vs. selected trace and rare earth elements in bulk-rock peridotite samples of the Jijal Complex. Primitive mantle fields are from [Palme and O'Neill \(2003\)](#). Abyssal and forearc peridotite fields are from [Niu et al. \(1997\)](#) and [Parkinson and Pearce \(1998\)](#), respectively.

compositions of olivine vary significantly, whereas the Cr# values of the chromite remain comparatively constant (Fig. 11a). The coarse-grained nature (Fig. 4), extensive high-temperature deformation, and extremely magnesian character of the Jijal peridotites preclude an origin as magma chamber cumulates. It is conceivable that the inferred high melt flux in the Jijal Complex peridotites was sufficient to broadly homogenize the composition of the several generations of Cr spinels (see following explanation). The Al_2O_3 versus TiO_2 contents of clinopyroxene in all the peridotite and chromitite samples (harzburgites, dunites, chromitites) show variation consistent with an increase in the degree of partial melting of their host rocks (Fig. 11b). However, the Cr# and Mg# values of the spinels correlate negatively, signifying that their host peridotites were formed by different degrees of partial melting. The spinel Cr#s and olivine Mg#s correlation to each other in the Jijal Complex peridotites indicate that the our analyzed samples are consistent with the olivine-spinel mantle array of [Arai and Miura \(2016\)](#). Jijal Complex peridotites are the residues of almost similar degrees of melt extraction because of this trend confirmation (Fig. 11c). The harzburgites of the Jijal Complex are residues of high degrees of partial melting (about 35–40%), whereas the dunites reflect about 40–43% partial melting. The massive, semi-massive and disseminated chromitites are not within the olivine-spinel mantle array.

Using the Cr#s content of magnesiochromite, the extent of fractional melting extent F (%) can be solved quantitatively using the following equation of [Hellebrand et al. \(2001\)](#).

$$F = 10 \times \ln(\text{Cr}\#) + 24$$

Where Cr# is the combination of $\text{Cr}/(\text{Cr} + \text{Al})$ of magnesiochromite. The Cr#s range from 0.71 to 0.72 in the magnesiochromite grains of Jijal Complex harzburgites, indicating that the lowest degree of melting (F_{\min}) is 20.5% for these rocks, whereas Cr#s in magnesiochromite of the dunites are 0.73–0.74, indicating that their F_{\min} is 20.9%. We conclude, therefore, that both the dunites and harzburgites of the Jijal

Complex are residues of high-degree partial melting. Other residues may have formed by higher degrees of partial melting or melt-rock reaction.

In order to better understand the partial melting of the Jijal Complex peridotites, we have modelled the REE compositions of whole-rock samples and clinopyroxene from the peridotites with a non-modal fractional melting model of [Johnson et al. \(1990\)](#) (Fig. 9a, c). This model comprises an assemblage consisting of olivine, orthopyroxene, clinopyroxene, spinel, which are used as the starting minerals as suggested in [Niu et al. \(1997\)](#). The partition coefficients used in this modelling may be affected by pressure, temperature and whole-rock composition. However, we assume that the partition coefficients are constant due to the complex relationships between the partition coefficients and the system environment.

The mineralogical and geochemical compositions of the depleted Jijal peridotites are taken to indicate that they are residues of mantle produced by multiple episodes and different degrees of partial melting. Mineralogical and petrological observations supporting this inference include: (1) Progressive depletion of the magmaphile major oxides of the studied peridotites (e.g., Al_2O_3 , CaO; Table S6; Fig. 7), and of the incompatible trace elements (e.g., Co, Yb, V, Sc, Y, Lu; Table S6; Fig. 8); (2) the olivine grains are forsterite (Fig. 5a–b); (3) the observed decrease of Al_2O_3 in both orthopyroxene and clinopyroxene from harzburgite to dunite (Fig. 5c–e); and (4) the large range of Cr# in the chromian spinel (Fig. 5g). The REE patterns of Jijal peridotites are compared with those predicted from petrological modelling in Fig. 9. The mantle metasomatism did not affect the concentrations of trace element such as Sc, Ti, V, Y and HREEs which are generally considered by the subduction conservative elements or fluid immobile elements ([Bizimis et al., 2000](#); [Niu, 2004](#); [Parkinson and Pearce, 1998](#)). Therefore, the HREE concentration can be used to estimate the degree of partial melting of the Jijal Complex peridotites. In wide-ranging, the HREE concentration of our samples is consistent with the results of REE modelling. The Jijal harzburgites have low HREE contents, indicating

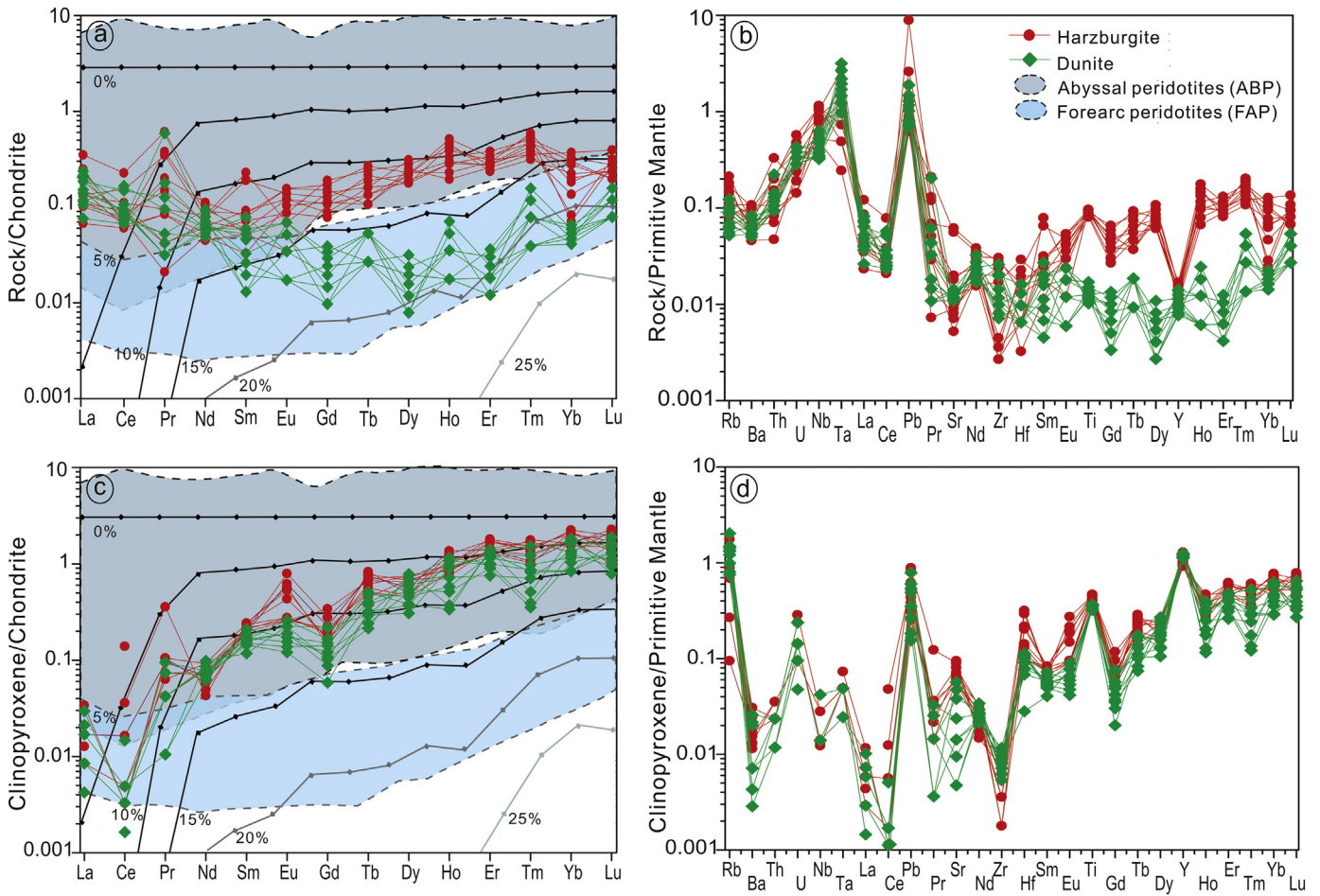


Fig. 9. (a) Chondrite-normalized rare earth element (REE) patterns for representative harzburgite and dunite samples from the Jijal Complex (normalizing values are from Sun and McDonough (1989)); (b) Primitive mantle-normalized trace element spider diagrams for representative harzburgite and dunite samples from Jijal Complex (normalizing values are from McDonough and Sun (1995)); (c) Chondrite-normalized REE patterns for representative harzburgite and dunite clinopyroxene from the Jijal Complex (normalizing values are after from Sun and McDonough (1989)); (d) Primitive mantle normalized trace element spider diagrams for representative harzburgite and dunite clinopyroxene from the Jijal Complex (normalizing values are after from McDonough and Sun (1995). Abyssal peridotite data are from Niu et al. (1997). Forearc peridotite data are from Parkinson and Pearce (1998).

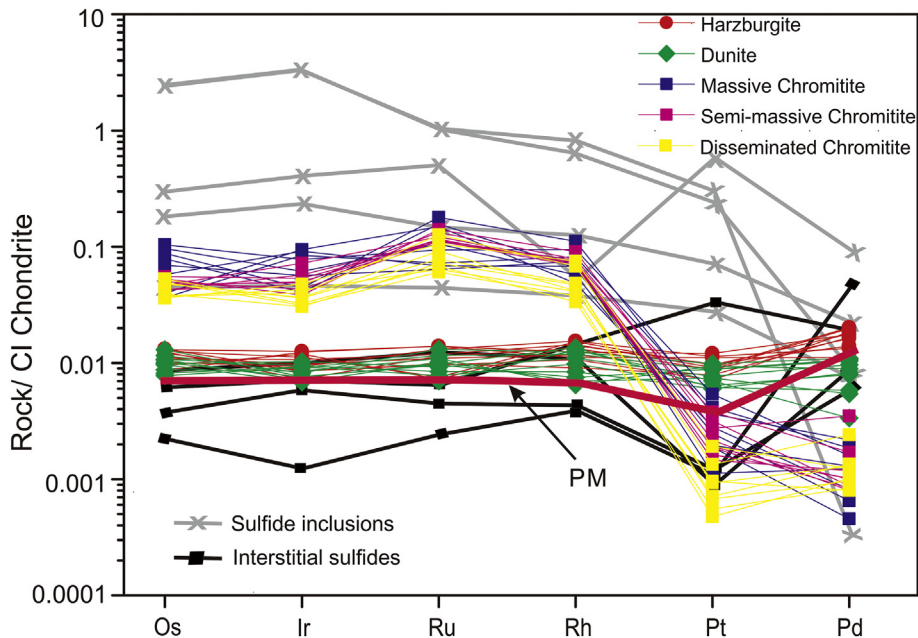


Fig. 10. Platinum group element (PGE) chondrite-normalized patterns for representative harzburgite, dunite and chromitite samples from the Jijal Complex. Data for sulfide inclusions and interstitial sulfides are from Alard et al. (2000). Chondrite values are from Sun and McDonough (1989). PM-primitive mantle.

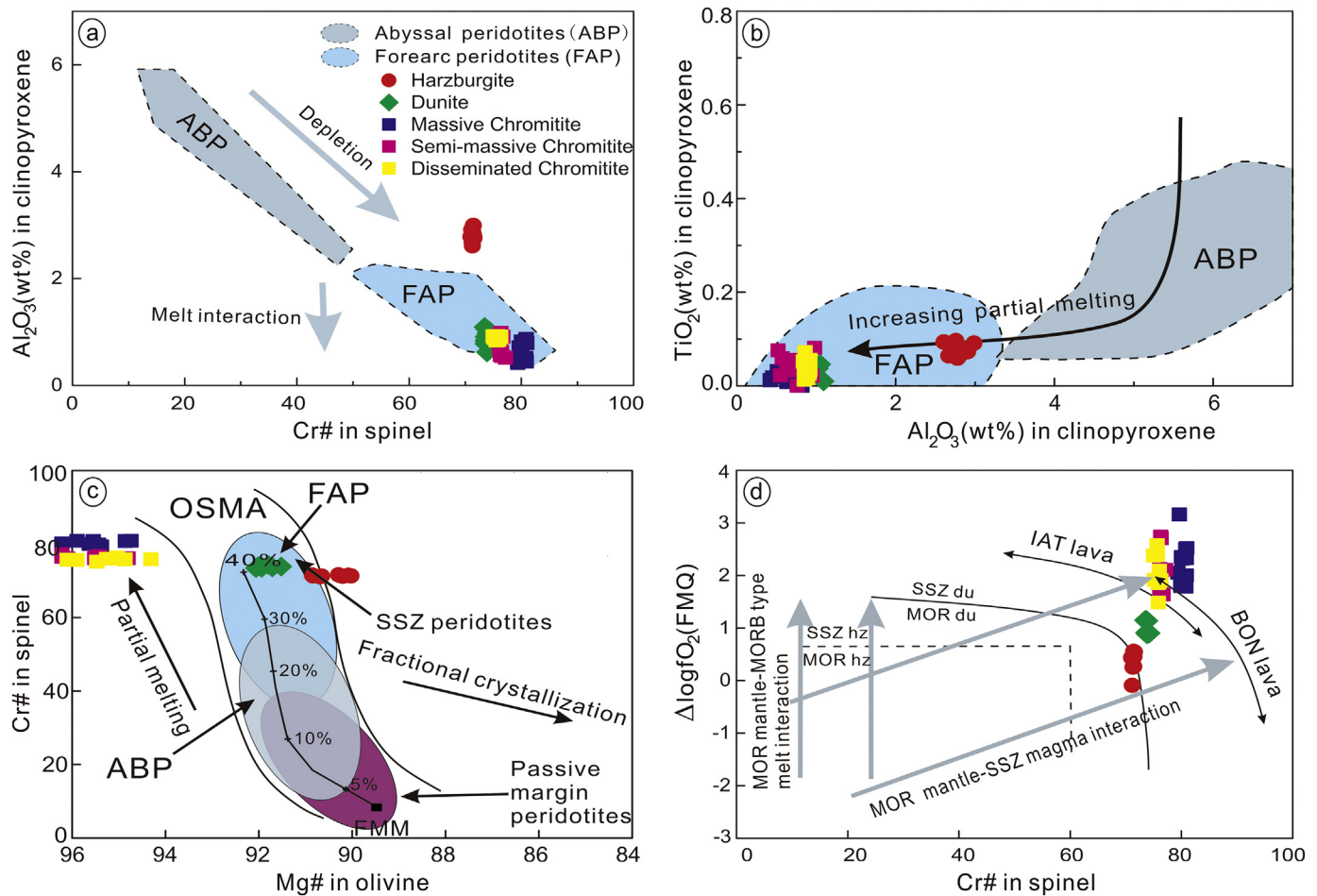


Fig. 11. (a) Bivariate diagram of Al_2O_3 (wt%) contents of clinopyroxene (Cpx) versus Cr# [100Cr / (Cr + Al)] of coexisting spinel from the Jijal Complex. The abyssal peridotite (ABP) and forearc peridotite (FAP) fields and the trends are from Pagé et al. (2008); (b) TiO_2 versus Al_2O_3 contents in clinopyroxene from the Jijal Complex peridotites and chromitites; (c) Cr# of chromite versus Mg# [100 Mg / (Mg + Fe²⁺)] of coexisting olivine from the Jijal peridotites; diagram is from Wu et al. (2017). Passive margin peridotites, ABP, and FAP fields and the trends are from Lian et al. (2016 and references therein). The degrees of melt extractions are calculated on the basis of spinel compositions using the empirical formula of Hellebrand et al. (2001). OSMA-olivine spinel mantle array; FMM-fertile mid-ocean range mantle; (d) Plot of $\Delta \log f_{\text{O}_2}$ (FMQ-fayalite-magnetite-quartz buffer) versus Cr# of spinels from the Jijal Complex dunites (du), harzburgites (hz) and chromitites. MOR (mid-ocean ridge) and SSZ (suprasubduction zone) discrimination boundaries for dunites (solid line) and harzburgites (dashed line) are shown. MORB-mid-ocean ridge basalt; BON-boninite; IAT-island arc tholeiite fields are from Parkinson and Pearce (1998).

10–15% partial melting (Fig. 9a, c). In contrast, the dunites appear to have undergone 20–25% melting and the harzburgite again went up to 20% partial melting to join the dunite field. These partial melting degrees broadly agree with those deduced from the magnesiochromites Cr# contents and olivine Mg# values (Fig. 11c). Although the HREE contents of the Jijal peridotites can be modelled effectively, their LREE contents are much higher than the values that can be explained by such a model; therefore we conclude that these harzburgites and dunites are not simply residues after different partial melting degrees.

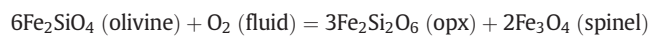
8.2. Oxygen fugacity (f_{O_2}) of the chromitites and peridotites

The mantle wedges above subduction zones are generally more oxidized than other tectonic setting of the mantle (Ballhaus et al., 1990; Parkinson and Pearce, 1998). During subduction of oceanic lithosphere, water derived from the subducted slab plays a major role in conversion of ferrous iron to ferric iron in melt (Wu et al., 2017) and in the formation of subduction-related melts.

The f_{O_2} of podiform chromitites and their associated peridotites magma systems can be readily assessed by using the thermometers of coexisting chromian spinel (Mg–Fe exchange), olivine and orthopyroxene (opx) in peridotites (Ballhaus et al., 1990; Wu et al., 2017). The paucity of orthopyroxene in chromitites and dunites, and

the intense serpentinization of most tectonized harzburgites, makes it difficult to estimate f_{O_2} in the mantle. Here we estimated the oxidation state of the Jijal chromitites and the associated dunites and harzburgites using the coexisting olivines and chromian spinel grains.

In order to calculate the values of f_{O_2} on the basis of microprobe analyses of the minerals, we used the formula of Ballhaus et al. (1990), which is based on the following reaction;



The f_{O_2} values have been calculated on the average mineral compositions basis which are given in electronic supplement (Table S9), as deviations ($\Delta \log f_{\text{O}_2}$ FMQ) from the FMQ (fayalite-magnetite-quartz) buffer (Fig. 11d). The calculated f_{O_2} values of all the studied samples are over the FMQ buffer; the massive chromitites show the most oxidized values with log units ranging from +1.79 to +3.16, followed by the semi-massive chromitites with values of +1.64 to +2.74, and disseminated chromitites with values of +1.49 to +2.57. The harzburgites and dunites have values of –0.09 to +0.55 and +0.88 to +1.15, respectively (Table S9). In summary, nearly all of the examined harzburgite, dunite and chromitites are from low to highly oxidized in Jijal Complex (Fig. 11d), with oxidation states low to high comparable with those of oceanic arc peridotites, which are roughly equivalent to

those of SSZ mantle wedges (Parkinson and Pearce, 1998; Pearce et al., 2000). It is noteworthy that the dunites and podiform chromitites in Jijal Complex have higher Cr# and fO_2 values than the associated harzburgites. The increase both in fO_2 and Cr#s of chromian spinel from harzburgites → dunites → disseminated chromitites → semi-massive chromitites → massive chromitites have been explained by interaction between the residual mantle harzburgite (that have back arc basin or MOR characteristics) and SSZ melts (that have higher fO_2 and Cr# contents) to generate chromitites and dunites due to the hydrous nature of the SSZ melts (that possess higher fO_2 and Cr# contents) (Parkinson and Pearce, 1998; Pearce et al., 2000; Uysal et al., 2009).

8.3. Melt-peridotite interaction, mantle metasomatism, and light rare earth element (LREE) enrichment

Magnesiocromites of the Jijal harzburgites have Cr#s of 71.2 to 71.6 and low TiO_2 contents of 0.052 to 0.122 wt%. In contrast, magnesiocromites in the chromitites, which are magmatic grains crystallized from high-Cr melts, have high Cr#s of 75.0–81.0 and high TiO_2 contents of 0.073–0.178 wt% (Fig. 5h). The high-Cr chromitites (Cr# >60) are typically surrounded by dunite envelopes in the field. In general, the abundance of clinopyroxene in the associated peridotites decreases adjacent the high-Cr chromitites, which we attribute to incongruent melting of clinopyroxene due to interaction between the upper mantle peridotites and a boninitic melt, as suggested by previous studies (Dilek and Morishita, 2009; Morishita et al., 2011; Pearce et al., 2000; Wu et al., 2017). In this model, the high-Cr chromitites are indicators of a high degree of partial melting, producing olivine and SiO_2 -rich boninitic melts. Dunitic peridotites are usually associated with irregular melt channels.

In the Jijal Complex TiO_2 contents of the magnesiocromites are very low because of the high MgO contents of the parental magmas (Fig. 5h). In contrast, the Cr# of the magnesiocromite increases from harzburgites to dunites and then to chromitites. In this situation, boninitic melt changed the composition of Al-rich spinels in the peridotites, leading to the crystallization of high-Cr chromitites. The Cr/Al ratio of spinels increased toward the chromitite body during the progress of this melt-peridotite interaction (González-Jiménez et al., 2011; Uysal et al., 2009). The highest Cr#s of spinels are recorded in boninites, a clear indication of their source from a highly refractory peridotite (Dilek and Morishita, 2009; González-Jiménez et al., 2011; Parkinson and Pearce, 1998). Thus, the clinopyroxene-rich samples in the peridotites are depleted to varying degrees due to interaction with boninitic melts and fluids. Based on the depleted harzburgite and dunite samples, it is concluded that this interpretation is also supported by a positive correlation between Cr# contents and fO_2 of the spinels (Fig. 11d), indicating that the spinel composition was affected by a melt-rock interaction (Pearce et al., 2000).

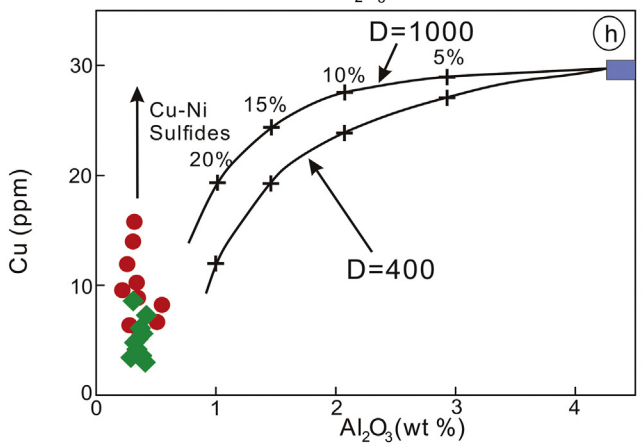
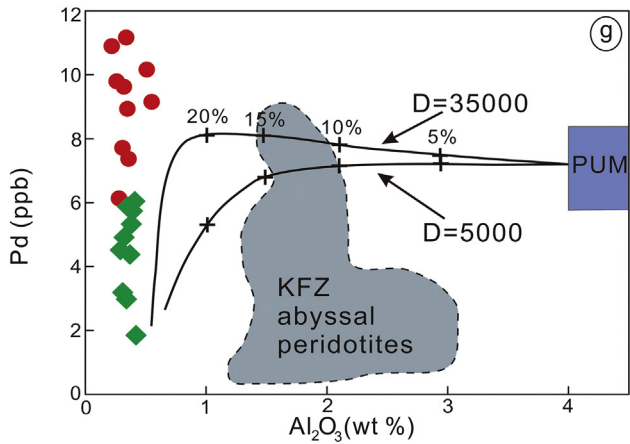
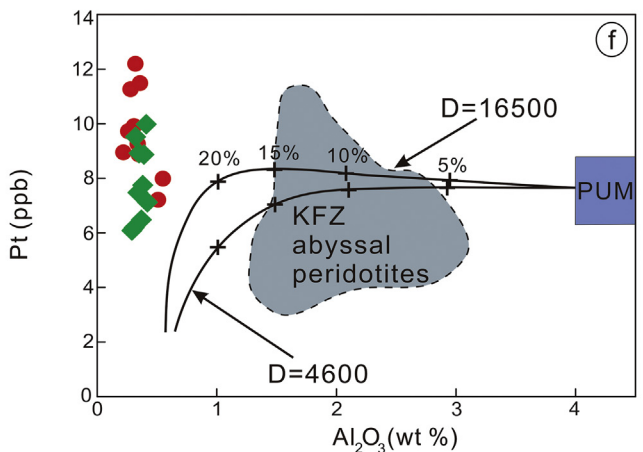
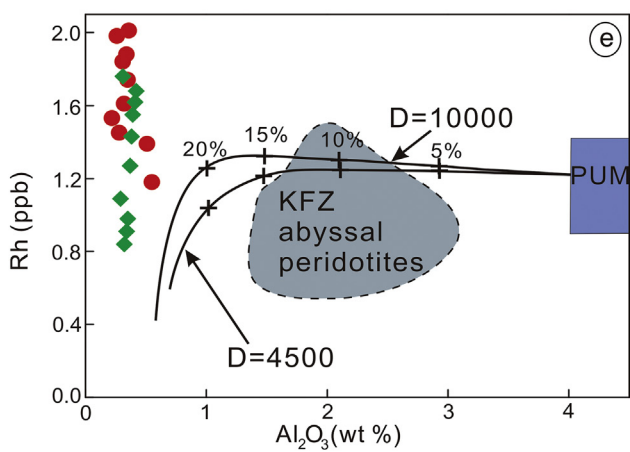
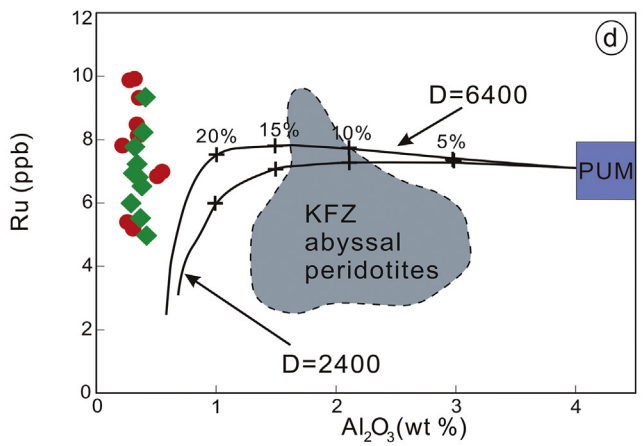
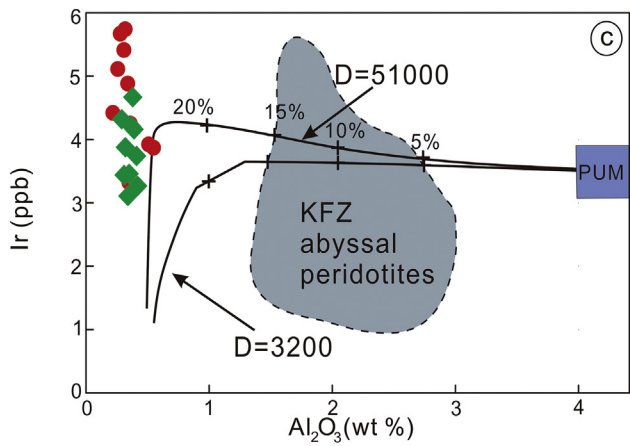
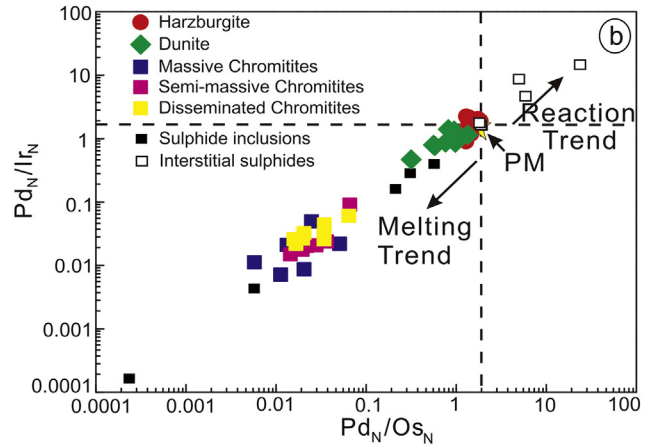
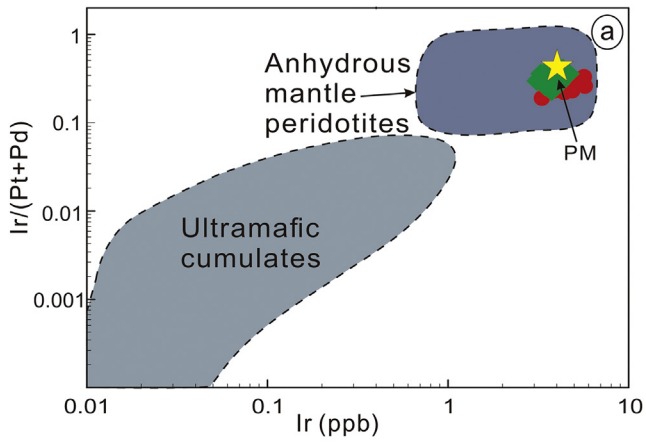
The Jijal harzburgites and clinopyroxenes from these harzburgites have spoon shaped, chondrite-normalized trace element patterns, showing notable LREE enrichment (Fig. 9a, c). This type of enrichment has commonly been interpreted as a major effect produced by interaction with subduction-derived fluids. However, these patterns are inconsistent with the modelled REE patterns, and but are well-matched with LREE enrichment (Fig. 9a-d) caused by interactions with water-rich SSZ magmas. This interaction is thought to occur in the cold thermal boundary layer, through which an earlier melt residue is affected by the ascending melts (Niu, 2004), resulting in enrichments both in LREE and high field strength elements (HFSE). The prominent LREE enrichment displayed by the Jijal peridotites was a result of their reaction with hydrous SSZ melts (Dilek and Furnes, 2014, 2011; Parkinson and Pearce, 1998) clearly indicating that these rocks are not simply melting residues (Saka et al., 2014; Zhou et al., 2005).

8.4. PGE constraints on melt-rock reaction

In mantle peridotites, the PGEs (Os, Ir, Ru, Rh, Pt and Pd) fractionate in a different way because of their different physical-chemical characteristics and melting temperatures during mantle melting and melt-rock interactions (Barnes et al., 2016; Lian et al., 2016, 2019; Luguet et al., 2007; Marchesi et al., 2013). Ir-group PGEs (IPGE: Os, Ir and Ru with melting temperature > 2000 °C) mostly occur in discrete minerals or sulfides, generally enclosed by chromite or silicate grains, whereas Pd-group PGEs (PPGE: Rh, Pt and Pd having melting temperature < 2000 °C) are normally hosted by interstitial sulfides in chromitites (Alard et al., 2000; Lian et al., 2019; Luguet et al., 2007; Woodland et al., 2002). The PPGEs are more easily accessed during partial melting (Woodland et al., 2002). The PPGE-rich interstitial sulfides are consumed firstly during partial melting of the mantle peridotites, resulting in IPGE enrichment in the residual peridotites comparative to PPGE which is depleted (Barnes et al., 2016; Lian et al., 2019; Luguet et al., 2007). From the modal mineralogy in mantle peridotites, the calculation of whole-rock PGEs concentrations are normally lower than measured concentrations, representing that 60–80% of the PGEs occur in sulfide-rich components (Alard et al., 2000; Luguet et al., 2007). Therefore, PGEs in the mantle peridotites are mainly hosted by sulfides and its compositions are the effective indicator of the degree of partial melting in mantle peridotites.

The Jijal Complex peridotites show depletions in Ir comparative to Os and Ru, and depletion in Pt comparative to Rh and Pd (Fig. 10). According to Alard et al. (2000), the depletion of Pt is consistent comparative to Rh and Pd with the PGEs affinity for interstitial sulfides. Because IPGEs remain in the mantle residues during initial partial melting, the high IPGE concentrations suggest that these rocks are refractory mantle peridotites. In the Ir-Ir/(Pt + Pd) diagram (Fig. 12a), all of the analyzed peridotite samples plot in the anhydrous mantle peridotite field, suggesting that they are partial melting residues rather than ultramafic cumulates (Barnes et al., 2016; Luguet et al., 2007; Marchesi et al., 2013). Because the melting of interstitial sulfides rich in Pd are easy to happen, the Pd/Ir ratios of the melt residue reveal the degree of partial melting (Woodland et al., 2002). The Jijal Complex peridotites Pd_N/Os_N and Pd_N/Ir_N ratios are much lower than the primitive mantle values because they have undergone variable degrees of partial melting (Fig. 12b). In the Pd_N/Os_N and Pd_N/Ir_N diagram, a Pd enrichment trend is apparent between the Jijal harzburgites and dunites, which was likely a result of melt-rock reaction (Alard et al., 2000). The lower Pd_N/Ir_N ratios of dunites compared to the harzburgites indicate that the dunites underwent higher degrees of partial melting than the harzburgites (Fig. 12b; Woodland et al., 2002).

Al_2O_3 is relatively compatible during alteration process, but tends to be incompatible in the process of mantle melting, and thus it can be used as an effective indicator of the mantle peridotites partial melting. PGEs are highly compatible in sulfides and its concentrations are affected by the abundance of sulfide phases during different stages of mantle melting (Barnes et al., 2016). The separation of sulfides from, or input into, the upper mantle may be a significant factor to determine the PGE contents of both mantle residues and melts (Barnes et al., 2016; Marchesi et al., 2013; Zhou et al., 2005). Marchesi et al. (2013), modelled the PGE and Cu behaviours against Al_2O_3 during the partial melting of primitive upper mantle using concentrations of McDonough and Sun (1995). Fig. 12c-h shows that the Jijal Complex harzburgite and dunite samples plot at the end of melting curve, consistent with the depleted modal mineralogy and chemical composition after high degree of partial melting. Although, the lack of correlation between Al_2O_3 , Cu and PGEs, and the presence of a Pt, Pd, Cu clear enrichment trend between the harzburgites and dunites suggest that the PPGE enriched sulfides must have crystallized between Jijal Complex peridotites and percolating melts due to reactions (Marchesi et al., 2013; Zhou et al., 2005). The PPGE enrichment patterns of the dunites are consistent with a melt-rock reaction origin. Thus, we postulate that the dunites



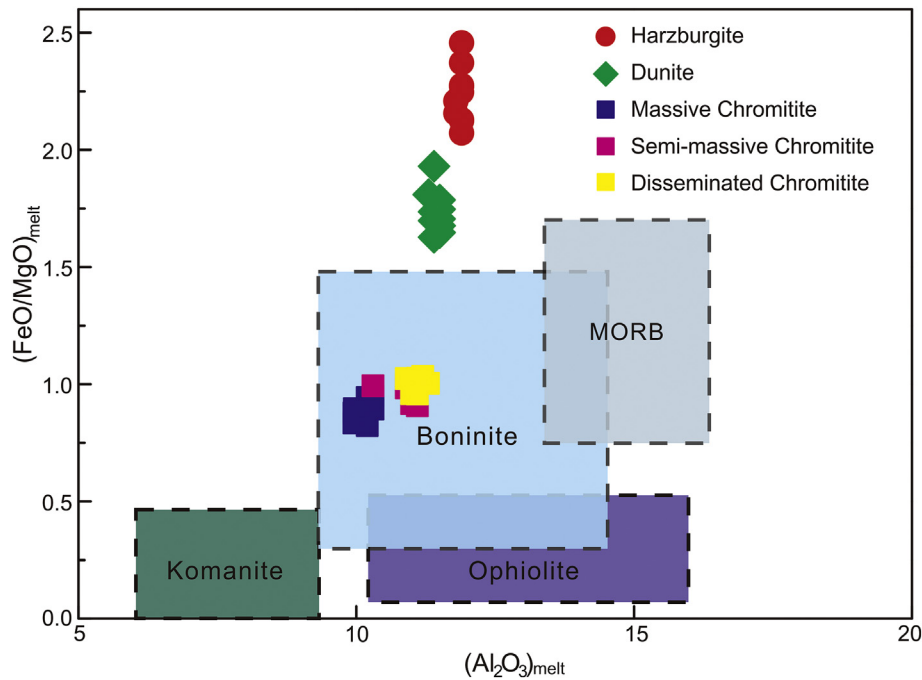


Fig. 13. $(\text{FeO}/\text{MgO})_{\text{melt}}$ versus $(\text{Al}_2\text{O}_3)_{\text{melt}}$ (wt%) diagram calculated on the basis of the whole-rock chemical compositions for rocks of the Jijal Complex. Tectonic discrimination fields are from Wu et al. (2017) and Ophiolite are the Tethyan Ophiolite field from Dilek et al. (2007) and Kakar et al. (2012, 2014). MORB—mid-oceanic ridge basalt. See text for discussion.

were formed by late-stage partial melting of harzburgites in a supra-subduction zone setting that produced boninitic magmas. In this late stage, incompatible PGEs (Rh, Pt and Pd especially) would be enriched in the boninitic melt due to additions from the subducted slab. So, the upper mantle would be enriched in these elements by the interaction with the boninitic melt (Fig. 12c–h).

Such boninitic melts may also be enriched in compatible PGEs, such as Os, Ir and Ru, by melting of pelagic sediments derived from the subducting slab, which commonly contain high concentrations of siderophile elements (e.g., Cu, Mo, and PGEs; (Alard et al., 2000; Marchesi et al., 2013; Woodland et al., 2002)). Therefore, these PGE compositions cannot be ascribed solely to melt extraction. Rather a slightly positive trend from Os to Pd (Fig. 10), which is not typical of the residual mantle material, suggests some degree of melt/rock reaction enrichment as discussed above. In the Jijal peridotites strong enrichment of Cu (Fig. 12h) suggests that these rocks underwent quite strong mantle metasomatism that caused precipitation of Cu–Ni sulfides in them (Alard et al., 2000; Lian et al., 2019; Marchesi et al., 2013).

8.5. Genesis of the Jijal chromitites

The chromitites in the Jijal Complex mainly occur in the upper mantle peridotites. These chromitites and spatially associated dunites are also common in many supra-subduction zone ophiolite, such as the Kop (Zhang et al., 2016), Luobusa (Zhou et al., 2005), Mirdita (Wu et al., 2017; Xiong et al., 2017), Muslim Bagh north-western Pakistan (Kakar et al., 2012, 2014), Oman (Rollinson and Adetunji, 2013) and Troodos (Greenbaum, 1977) ophiolites. The significant information based on geochemical signature of the chromite parental magmas and

tectonic environment of their genesis can be acquired by studying the composition of chromian spinels. Chromian spinels in cumulate rocks occur as either cumulus or intercumulus phases and are generally produced by crystallization of parental melts. Therefore, the chemical compositions of chromian spinel have been used by many researchers as a sensitive petrogenetic indicator to determine the parental melt composition (Arai and Miura, 2016; Dick and Bullen, 1984; Dilek and Furnes, 2014; Kamenetsky et al., 2001; Rollinson and Adetunji, 2013). Experimental research has revealed that Al_2O_3 and TiO_2 contents, as well as FeO/MgO ratios in chromian spinel, are directly related to the parental melt compositions (Kamenetsky et al., 2001; Maurel and Maurel, 1982). The Al_2O_3 content of chromian spinel is mainly controlled by the Al_2O_3 content of parental melt, which can be calculated by using the formula of Maurel and Maurel (1982):

Al_2O_3 (wt%) in chromian spinel = $0.035(\text{Al}_2\text{O}_3)^{2.42}$ (wt%) in parental melt.

So, the melt values of FeO/MgO can be calculated from the chromian spinel FeO/MgO values. By using empirical formula proposed by Maurel and Maurel (1982), the FeO/MgO ratios of the melt can be calculated for almost all types of chromitites with silicate matrix (i.e., massive, semi massive and disseminated chromitites), while Fe and Mg are balanced between chromian spinel and silicate minerals:

$$\ln(\text{FeO}/\text{MgO})_{(\text{spinel})} = 0.47 - 1.07\text{Al}\#_{(\text{spinel})} + 0.64\text{Fe}^{3+}\#_{(\text{spinel})} + \ln(\text{FeO}/\text{MgO})_{(\text{melt})}$$

with FeO and MgO in wt%, $\text{Al}\# = \text{Al}/(\text{Cr} + \text{Al} + \text{Fe}^{3+})$ and $\text{Fe}^{3+}\# = \text{Fe}^{3+}/(\text{Cr} + \text{Al} + \text{Fe}^{3+})$.

Fig. 12. (a) Plot of whole-rock $\text{Ir}/(\text{Pt} + \text{Pd})$ vs Ir for Jijal peridotites. PM—primitive mantle; (b) Chondrite-normalized Pd_N/Ir_N versus Pd_N/Os_N for rocks of the Jijal Complex; fields of anhydrous mantle peridotites and ultramafic cumulates are from Deschamps et al. (2013). Sulfide inclusions and interstitial sulfides for platinum group element (PGE) contents and trends are from Alard et al. (2000). Chondrite values are from Sun and McDonough (1989). Primitive mantle values from McDonough and Sun (1995); (c) Plot of Ir versus Al_2O_3 for the Jijal Complex peridotites. KFZ—Kane Fracture Zone, Atlantic Ocean; PUM—primitive upper mantle; D—Nernst partition coefficient; (d) Ru versus Al_2O_3 for Jijal peridotites and dunites; (e) Rh versus Al_2O_3 for Jijal peridotites and dunites; (f) Pt versus Al_2O_3 for Jijal peridotites and dunites; (g) Pd versus Al_2O_3 for Jijal peridotites and dunites; (h) Cu versus Al_2O_3 for Jijal peridotites and dunites. Fields of KFZ, abyssal peridotites, and primitive mantle values and melting curves are from Marchesi et al. (2013). See text for discussion.

The calculated results for the Jijal chromitites show that the FeO/MgO ratios of the parental magmas from which the massive, semi-massive, disseminated chromitites, harzburgites, and dunites crystallized are 0.82–0.95, 0.91–1.01, 0.96–1.03, 2.07–2.46, 1.63–1, respectively. The corresponding Al₂O₃ contents are 939.96–10.3, 10.3–11.1, 10.9–11.3, 11.8–11.9 and 11.3–11.5 wt%, respectively. The FeO/MgO ratios are similar to those observed in boninitic rocks (Table S5; Fig. 13) (Wilson, 1989). The composition of calculated parental magma shows a good fit in boninitic field melts with comparison to that of primitive magmas from various tectonic settings (Fig. 13). According to Mondal et al. (2006), the high Cr#s and high water contents of boninitic magmas allow the early crystallization of spinel relative to Cr-rich pyroxene and subsequently the crystallization of large amount of Cr-rich spinels. The parental melt compositions of the chromian spinel of the Jijal chromitites closely resemble those of boninites of Bonin Island, Japan (Hickey and Frey, 1982). Similar melts with boninitic affinities are considered to have been responsible for the high-Cr chromitites formation from many localities such as Bay of Bengal Rutland Island (Ghosh et al., 2009), Eastern Cuba Mayari Cristal ophiolite (González-Jiménez et al., 2011), Iran Sorkhband ultramafics (Najafzadeh et al., 2008), Kazakhstan Kempirsai ophiolite (Melcher et al., 1997), Turkish-Muğla and Aladag ophiolites (Lian et al., 2019; Uysal et al., 2009).

It has been broadly accepted that chromitites of high-Cr (Cr# > 60) are generated from boninitic melts, whereas chromitites of high-Al (Cr# < 60) form from less refractory, MORB-like arc tholeiitic magmas (Arai and Yurimoto, 1994; Wu et al., 2017; Xiong et al., 2017). Our results are consistent with these models and indicate that the parental melts of the chromitites are boninites generated in a forearc tectonic setting (Fig. 13). Experimental studies suggest that chromite precipitation is triggered by melt-peridotite reaction, a process that requires high temperatures, low pressures (0.3–1.04 Pa) and abundant water (Glenn and Timothy, 1998; Klingenberg and Kushiro, 1996; Van der

Laan et al., 1989). These conditions are typically found during subduction initiation in SSZ environments (Dilek and Flower, 2003; González-Jiménez et al., 2011; Kakar et al., 2012, 2014; Van der Laan et al., 1989; Garrido et al., 2007).

8.6. Geodynamic setting of the Jijal Complex chromitites and peridotites

Island-arc and back-arc settings are the widely accepted environments for podiform chromitite formation (Rollinson and Adetunji, 2013; Uysal et al., 2009; Zhou et al., 2005). In these environments, the lithologies of the upper mantle interact with the migrating magma produced at highly depth may forming chromitites body (Arai and Yurimoto, 1994; Zhou et al., 2014). Spinel compositions in chromitites and peridotites also reveal valuable information on the composition of their parental melts and the geodynamic setting in which they crystallized (Dick and Bullen, 1984).

Here we present a tectono-magmatic model for the melt evolution, based on field observations together with the geochemical characteristics of chromitites and associated peridotites of the Jijal Complex to constrain the tectonic setting of the Indus Suture Zone Ophiolites (Fig. 14). Recognition of an early magmatic events of boninitic extraction (marked by depletion of REE) in the ultramafic section of Jijal complex lends support to a model involving subduction initiation in a SSZ environment (Dilek and Flower, 2003; González-Jiménez et al., 2011; Kakar et al., 2012, 2014). In the northern Pakistan, Kohistan Arc Complex (KAC) represents an early Cretaceous intra-oceanic arc exhumed unit which is formed during Neo-Tethys Ocean subduction along the north underneath Karakorum Plate (Burg et al., 1998; Schaltegger et al., 2002). This complex is now sandwiched between the Indian plate to the south and Karakoram (Asian) plate to the north, and is separated from these blocks, respectively, by the Main Mantle Thrust (MMT, or Indus Suture) and Main Karakoram Thrust (MKT). The Jijal ultramafic complex, present on the hanging wall of the MMT, showing the

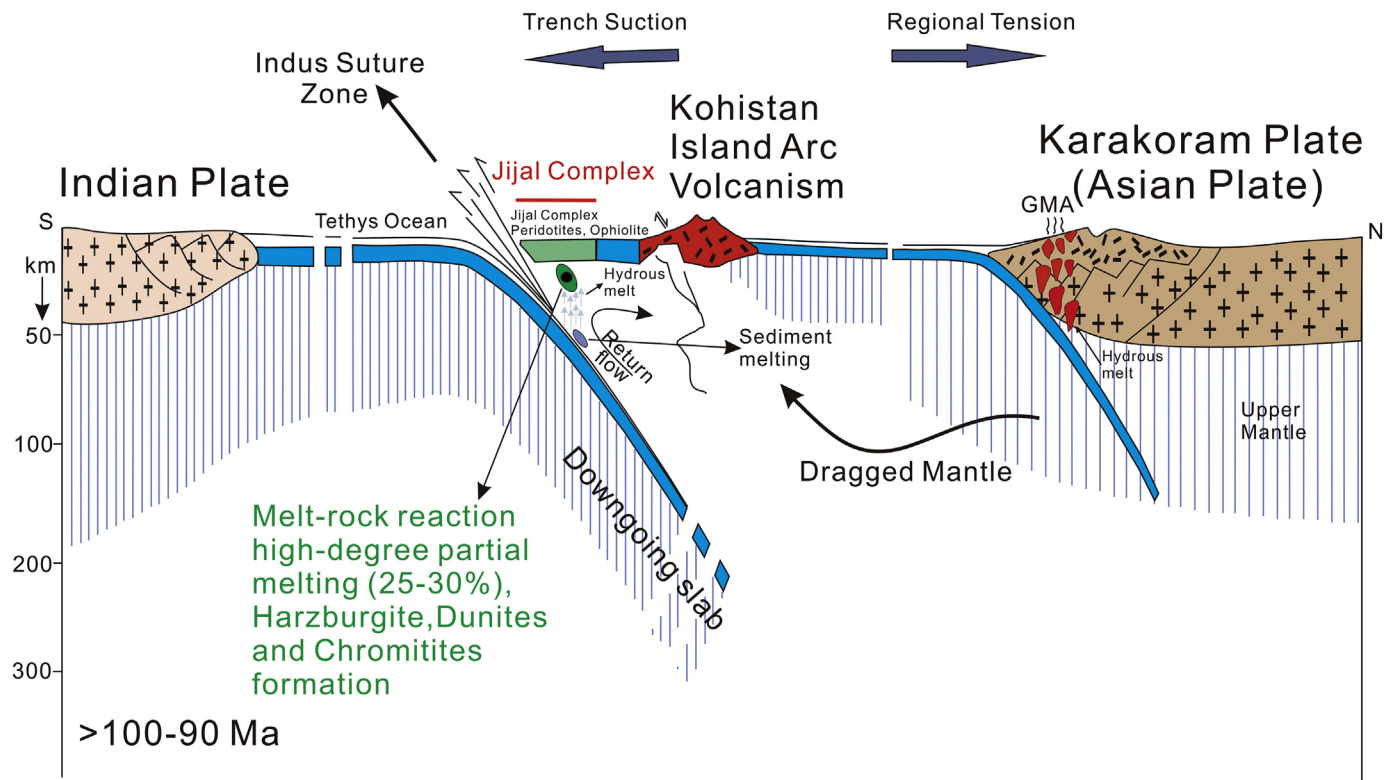


Fig. 14. Tectonic model for the melt evolution of the harzburgite and dunite-chromitite occurrences in the Jijal Complex Ophiolite along the Main Mantle Thrust (MMT or Indus Suture Zone), North Pakistan (modified after Schaltegger et al. (2002); Dilek and Furnes (2011, 2014), GMA-Gangdese Magmatic Arc, See text for discussion).

KAC ultramafic roots that were shaped during the arc building stage (ca. 110–90 Ma, see [Schaltegger et al., 2002](#); [Faisal et al., 2014, 2016](#)).

The Jijal complex has subsequently passed through complex episodes. After formation, it was subducted to substantial depth beneath the island arc and was then uplifted to its present location along the MMT ([Jan and Howie, 1981](#)) ([Fig. 14](#)). These events must have had important effects on the mineral phases, especially Cr-spinel.

The Jijal complex is composed of an ultramafic section with peridotite (PEZ) and pyroxenite (PYZ) zones ([Burg et al., 1998](#); [Yamamoto and Yoshino, 1998](#)). Our mineralogical and geochemical data show that the Jijal peridotites are the depleted mantle residues after relatively high degrees of partial melting ([Fig. 14](#); 25–30%) of already depleted, upwelling asthenospheric mantle. The melting was triggered by dehydration of the sinking oceanic lithosphere and resulted in enrichment of LREE and HFSE in the peridotites by interaction of ascending decompressional melts with the earlier melt residues. During subduction, the slab-derived melts/fluids were released into the mantle wedge, triggering a higher degree (25–30%) of partial melting of the peridotites at shallow depth. The unusually depleted nature of the forearc peridotites requires unusual melting conditions: abnormally high temperatures, high volatile flux, or both. Highly depleted dunites and chromitites in ophiolites are cumulates and hence genetically related, and they should reflect the same degree of partial melting as the source melts of the mantle wedge overlying the subduction zone. This high-degree, low-pressure–high-temperature partial melting of highly depleted harzburgites produced olivine- and SiO₂-rich boninitic melts (enriched in incompatible PGEs and Cu–Ni sulfides) that reacted with the peridotites, forming the podiform chromitite deposits surrounded by dunite envelopes. Partial melting of pelagic sediments in the subduction zone along Indus Suture Zone ([Fig. 14](#)) produced silica saturated melts that react with hot, hydrous depleted peridotites to produce boninitic melts/fluids ([Dilek et al., 2008](#)) with high concentrations of Cu, Mo, and PGEs, which played an important role in the mantle metasomatism and enrichment. The incompatible element-enriched boninitic melts percolating through the dunites precipitated Cu–Ni sulfides in melt channels. Progressive evolution of melts at this stage of formation of the Jijal Complex generated the cumulates and overlying extrusive rocks with boninite geochemical affinities ([Arif and Jan, 2006](#)).

9. Conclusions

Mineralogical modal, mineral compositions and bulk-rock geochemistry of the upper mantle peridotites from the Jijal Complex ophiolite in northern Pakistan indicate high partial melting degrees and show resemblance to forearc peridotites formed during the subduction initiation. Cr-rich podiform chromitites formed as a result of reaction between subduction-generated fluids and melts and the previously depleted peridotites of mantle wedge under high-temperature, low-pressure conditions. These processes generally produced boninitic magmas enriched in incompatible PGEs and Cu–Ni sulfides that penetrated the dunitic peridotites along irregular melt channels. LREE-enrichment of the Jijal Complex ophiolitic mantle peridotites also indicate that these rocks were metasomatized by LREE-enriched fluids derived from subduction slab. The peridotites reflect a complex history involving partial melting, depletion, enrichment, and magmatism-metasomatism during evolution of the Early Cretaceous Tethyan oceanic lithosphere in a forearc spreading setting during subduction initiation.

The mineral and whole-rock geochemistry of the chromitite and dunite along with their impregnation-related microtextures, are similar to those of chromite crystallized from tholeiite to boninite melts. Most of the massive, semi-massive and disseminated chromitites have high Cr values (70–80 and above), but there are systematic compositional changes in olivines and magnesiochromites from harzburgite to dunite envelopes to massive chromitite, likely reflecting melt-rock reactions. These chromitites are highly depleted in PPGE and enriched in IPGE,

both features being well-recognized in the worldwide ophiolitic podiform chromitites. The PGEs abundances in the Jijal Complex peridotites resemble strongly depleted mantle rocks and indicates high partial melting degrees (25–30%) in the mantle source. Taken together, our new mineralogical and geochemical data suggest that the Jijal Complex Ophiolite formed along Indus Suture Zone in a mantle wedge of supra-subduction zone, in which the composition of magma gradually changed with time.

Supplementary data to this article can be found online at <https://doi.org/10.1016/j.lithos.2020.105566>.

Declaration of Competing Interest

The authors declared that there is no conflict of interest.

Acknowledgements

We express our sincere thanks to Prof. Dr. Muhammad Tahir Shah (Vice Chancellor) FATA University, Tribal Subdivision Darra Kohat, Pakistan, for their assistance for the fieldwork logistics, and State Key Laboratory of Geological Processes and Mineral Resources, China University of Geosciences Wuhan for the geochemical analysis. We are grateful to Amjad Hussain, Dongyang Lian and Qiu Tian for insightful discussion on the petrology of upper mantle peridotites. We thank Prof. Dr. Yildirim Dilek (Miami University, USA) and an anonymous reviewer for their useful comments and suggestions which helped improve the presentation of the manuscript. This study was financially supported by grants from the National Natural Science Foundation of China (No. 41325007) and State Key Laboratory of Geological Processes and Mineral Resources (MSFGPMR03). This is contribution 26 from Center for Research in Economic Geology and Exploration Targeting (CREGET) with China University of Geosciences (Wuhan).

References

- Alard, O., Griffin, W.L., Lorand, J.P., Jackson, S.E., O'Reilly, S.Y., 2000. Non-chondritic distribution of the highly siderophile elements in mantle sulphides. *Nature* 407, 891–894.
- Alonso-Perez, R., Müntener, O., Ulmer, P., 2009. Igneous garnet and amphibole fractionation in the roots of island arcs: Experimental constraints on andesitic liquids. *Contrib. Mineral. Petrol.* 157, 541–558.
- Arai, S., Miura, M., 2016. Formation and modification of chromitites in the mantle. *Lithos* 264, 277–295.
- Arai, S., Yurimoto, H., 1994. Podiform chromitites of the Tari-Misaka ultramafic complex, southwestern Japan, as mantle–melt interaction products. *Econ. Geol.* 89, 1279–1288.
- Arai, S., Kadoshima, K., Morishita, T., 2006. Widespread arc-related melting in the mantle section of the northern Oman ophiolite as inferred from detrital chromian spinels. *J. Geol. Soc. London.* 163, 869–879.
- Arif, M., Jan, M.Q., 2006. Petrotectonic significance of the chemistry of chromite in the ultramafic-mafic complexes of Pakistan. *J. Asian Earth Sci.* 27, 628–646.
- Ballhaus, C., Berry, R.F., Green, D.H., 1990. Oxygen fugacity controls in the Earth's upper mantle. *Nature* 348, 437–440.
- Barnes, S.J., Pagé, P., Prichard, H.M., Zientek, M.L., Fisher, P.C., 2016. Chalcophile and platinum-group element distribution in the Ultramafic series of the Stillwater complex, MT, USA—implications for processes enriching chromite layers in Os, Ir, Ru, and Rh. *Miner. Depos.* 51, 25–47.
- Bizimis, M., Salters, V.J.M., Bonatti, E., 2000. Trace and REE content of clinopyroxenes from supra-subduction zone peridotites. Implications for melting and enrichment processes in island arcs. *Chem. Geol.* 165, 67–85.
- Burg, J.P., Bodinier, J.L., Chaudhry, S., Hussain, S., Dawood, H., 1998. Infra-arc mantle–crust transition and intra-arc mantle diapirs in the Kohistan complex (Pakistani Himalaya): Petro-structural evidence. *Terra Nova* 10, 74–80.
- Derbyshire, E.J., O'Driscoll, B., Lenaz, D., Zanetti, A., Gertisser, R., 2019. Chromitite petrogenesis in the mantle section of the Ballantrae Ophiolite complex (Scotland). *Lithos* 344–345, 51–67.
- Deschamps, F., Godard, M., Guillot, S., Hattori, K., 2013. Geochemistry of subduction zone serpentinites: a review. *Lithos* 178, 96–127.
- Dick, H.J.B., Bullen, T., 1984. Chromian spinel as a petrogenetic indicator in abyssal and alpine-type peridotites and spatially associated lavas. *Contrib. Mineral. Petrol.* 86, 54–76.
- Dilek, Y., Flower, M.F.J., 2003. Arc-trench rollback and forearc accretion: 2. A model template for ophiolites in Albania, Cyprus, and Oman. *Geol. Soc. London. Spec. Publ.* 218, 43–68.
- Dilek, Y., Furnes, H., 2011. Ophiolite genesis and global tectonics: Geochemical and tectonic fingerprinting of ancient oceanic lithosphere. *Geol. Soc. Am. Bull.* 123, 387–411.

- Dilek, Y., Furnes, H., 2014. Ophiolites and their origins. *Elements* 10, 93–100.
- Delik, Y., Furnes, H., 2019. Tethyan ophiolites and Tethyan seaways. *Geol. Soc. London* 176, 899–912. <https://doi.org/10.1144/jgs2019-129>.
- Dilek, Y., Morishita, T., 2009. Melt migration and upper mantle evolution during incipient arc construction: Jurassic Eastern Mirdita ophiolite, Albania. *Isl. Arc* 18, 551–554.
- Dilek, Y., Robinson, P.T., 2008. Ophiolites in earth history: introduction. *Geol. Soc. Lond. Spec. Publ.* 218, 1–8.
- Dilek, Y., Thy, P., 1998. Structure, petrology and seafloor spreading tectonics of the Kizildag Ophiolite, Turkey. *Geol. Soc. Spec. Publ.* 148, 43–69.
- Dilek, Y., Yang, J., 2018. Ophiolites, diamonds, and ultrahigh-pressure minerals: New discoveries and concepts on upper mantle petrogenesis. *Lithosphere* 10, 3–13.
- Dilek, Y., Furnes, H., Shallo, M., 2007. Suprasubduction zone ophiolite formation along the periphery of Mesozoic Gondwana. *Gondw. Res.* 11, 453–475.
- Dilek, Y., Furnes, H., Shallo, M., 2008. Geochemistry of the Jurassic Mirdita Ophiolite (Albania) and the MORB to SSZ evolution of a marginal basin oceanic crust. *Lithos* 100, 174–209.
- El Ghorfi, M., Melcher, F., Oberthür, T., Boukhari, A.E., Maacha, L., Maddi, A., Mhaili, M., 2008. Platinum group minerals in podiform chromitites of the Bou Azzer ophiolite, Anti Atlas, Central Morocco. *Mineral. Petrol.* 92, 59–80.
- Faisal, S., Larson, K.P., Cottle, J.M., Lamming, J., 2014. Building the Hindu Kush: Monazite records of terrane accretion, plutonism and the evolution of the Himalaya-Karakoram-Tibet orogen. *Terra Nova* 26, 395–401.
- Faisal, S., Larson, K.P., King, J., Cottle, J.M., 2016. Rifting, subduction and collisional records from pluton petrogenesis and geochronology in the Hindu Kush, NW Pakistan. *Gondwana Res.* 35, 286–304.
- Fu, C., Yan, Z., Aitchison, J.C., Guo, X., Xia, W., 2019. Abyssal and suprasubduction peridotites in the Lajishan ophiolite belt: Implication for initial subduction of the prototethyan ocean. *J. Geol.* 127, 393–410.
- Gaetani, G.A., Grove, T.L., 1998. The influence of water on melting of mantle peridotite. *Contrib. Mineral. Petrol.* 131, 323–346.
- Garrido, C.J., Bodinier, J.L., Dhuime, B., Bosch, D., Chanefo, I., Bruguier, O., Hussain, S.S., Dawood, H., Burg, J.P., 2007. Origin of the island arc Moho transition zone via melt-rock reaction and its implications for intracrustal differentiation of island arcs: evidence from the Jijal complex (Kohistan complex, northern Pakistan). *Geology* 35, 683–686.
- Ghosh, B., Pal, T., Bhattacharya, A., Das, D., 2009. Petrogenetic implications of ophiolitic chromite from Rutland Island, Andaman – a boninitic parentage in supra-subduction setting. *Mineral. Petrol.* 96, 59–70.
- Glenn, A.G., Timothy, L.G., 1998. The influence of water on melting of mantle peridotite. *Contrib. Mineral. Petrol.* 131, 323–346.
- González-Jiménez, J.M., Proenza, J.A., Gervilla, F., Melgarejo, J.C., Blanco-Moreno, J.A., Ruiz-Sánchez, R., Griffin, W.L., 2011. High-Cr and high-Al chromitites from the Sagua de Tánamo district, Mayarí-Cristal ophiolitic massif (eastern Cuba): Constraints on their origin from mineralogy and geochemistry of chromian spinel and platinum-group elements. *Lithos* 125, 101–121.
- Greenbaum, D., 1977. The chromitiferous rocks of the Troodos ophiolite complex. *Cyprus. Econ. Geol.* 72, 1175–1194.
- Hart, S.R., Zindler, A., 1986. In search of a bulk-Earth composition. *Chem. Geol.* 57, 247–267.
- Hellebrand, E., Snow, J.E., Dick, H.J.B., Hofmann, A.W., 2001. Coupled major and trace elements as indicators of the extent of melting in mid-ocean-ridge peridotites. *Nature* 410, 677–681.
- Hickey, R.L., Frey, F.A., 1982. Geochemical characteristics of boninite series volcanics: implications for their source. *Geochim. Cosmochim. Acta* 46, 2099–2115.
- Jan, M.Q., Howie, R.A., 1981. The mineralogy and geochemistry of the metamorphosed basic and ultrabasic rocks of the jijal complex, Kohistan, NW Pakistan. *J. Petrol.* 22, 85–126.
- Johnson, K.T.M., Dick, H.J.B., Shimizu, N., 1990. Melting in the Oceanic Upper Mantle: an Ion Microprobe Study of Diopsides in Abyssal Peridotites. *J. Geophys. Res.* 95, 2661–2678.
- Kakar, M.I., Collins, A.S., Mahmood, K., Foden, J.D., Khan, M., 2012. U-Pb zircon crystallization age of the Muslim Bagh ophiolite: Enigmatic remains of an extensive pre-Himalayan arc. *Geology* 40, 1099–1102.
- Kakar, M.I., Kerr, A.C., Mahmood, K., Collins, A.S., Khan, M., McDonald, I., 2014. Supra-subduction zone tectonic setting of the Muslim Bagh Ophiolite, northwestern Pakistan: Insights from geochemistry and petrology. *Lithos* 202–203, 190–206.
- Kamenetsky, V.S., Crawford, A.J., Meffre, S., 2001. Factors Controlling Chemistry of Magmatic Spinel: an Empirical Study of Associated Olivine, Cr-spinel and Melt Inclusions from Primitive Rocks. *J. Petrol.* 42, 655–671.
- Khan, M., Kerr, A.C., Mahmood, K., 2007. Formation and tectonic evolution of the Cretaceous-Jurassic Muslim Bagh ophiolite complex, Pakistan: implications for the composite tectonic setting of ophiolites. *J. Asian Earth Sci.* 31, 112–127.
- Klingenberg, B.M.E.T., Kushiro, I., 1996. Melting of a chromite-bearing harzburgite and generation of boninitic melts at low pressures under controlled oxygen fugacity. *Lithos* 37, 1–14.
- Le Maitre, R.W., Streckeis, A., Zanettin, B., Le Bas, M.J., Bonin, B., Bateman, P., 2002. *Igneous Rocks: A Classification and Glossary of Terms (Recommendations of the IUGS Subcommission on the Systematics of Igneous Rocks)*. Cambridge Univ. Press, p. 239.
- Lian, D., Yang, J., Robinson, P.T., Liu, F., Xiong, F., Zhang, L., Gao, J., Wu, W., 2016. Tectonic Evolution of the Western Yarlung Zangbo Ophiolite Belt, Tibet: Implications from the Petrology, Mineralogy, and Geochemistry of the Peridotites. *J. Geol.* 124, 353–376.
- Lian, D., Yang, J., Dilek, Y., Rocholl, A., 2019. Mineralogy and geochemistry of peridotites and chromitites in the Aladag Ophiolite (southern Turkey): melt evolution of the cretaceous Neotethyan mantle. *J. Geol. Soc. London*. 176, 958–974.
- Llanes, A.I., Proenza, J.A., Zaccarini, F., Garuti, G., Santa Cruz Pacheco, M., 2015. Al- and Cr-rich chromitites from the Eastern Havana-Matanzas ophiolites (Western Cuba). *Epidiodes* 38, 334–343.
- Luguet, A., Lorand, J.P., Seyler, M., 2003. Sulfide petrology and highly siderophile element geochemistry of abyssal peridotites: a coupled study of samples from the Kane Fracture Zone (45°W 23°20N MARK Area, Atlantic Ocean). *Geochim. Cosmochim. Acta* 67, 1553–1570.
- Luguet, A., Shirey, S.B., Lorand, J.P., Horan, M.F., Carlson, R.W., 2007. Residual platinum-group minerals from highly depleted harzburgites of the Lherz massif (France) and their role in HSE fractionation of the mantle. *Geochim. Cosmochim. Acta* 71, 3082–3097.
- Mahmood, K., Boudier, F., Gnos, E., Monié, P., Nicolas, A., 1995. ⁴⁰Ar/³⁹Ar dating of the emplacement of the Muslim Bagh ophiolite, Pakistan. *Tectonophysics* 250, 169–181.
- Marchesi, C., Garrido, C.J., Harvey, J., González-Jiménez, J.M., Hidas, K., Lorand, J.P., Gervilla, F., 2013. Platinum-group elements, S, Se and Cu in highly depleted abyssal peridotites from the Mid-Atlantic Ocean Ridge (ODP Hole 1274A): Influence of hydrothermal and magmatic processes. *Contrib. Mineral. Petrol.* 166, 1521–1538.
- Maurel, C., Maurel, P., 1982. Etude expérimentale de la distribution de l'aluminium entre bain silicate basique et spinelle chromifère. Implications pétrogénétiques: teneur en chrome des spinelles. *Bull. Mineral.* 105, 197–202.
- McDonough, W.F., Sun, S., 1995. The composition of the Earth. *Chem. Geol.* 2541, 223–253.
- Melcher, F., Grum, W., Simon, G., Thalhammer, T.V., Stumpfl, E.F., 1997. Petrogenesis of the ophiolitic giant chromite deposits of Kempirsai, Kazakhstan: a study of solid and fluid inclusions in chromite. *J. Petrol.* 38, 1419–1458.
- Miller, C., Thöni, M., Frank, W., Schuster, R., Melcher, F., Meisel, T., Zanetti, A., 2003. Geochemistry and tectonomagmatic affinity of the Yungbwa ophiolite, SW Tibet. *Lithos* 66, 155–172.
- Mondal, S.K., Ripley, E.M., Li, C., Frei, R., 2006. The genesis of Archaean chromitites from the Nuasahi and Sukinda massifs in the Singhbhum Craton, India. *Precambrian Res.* 148, 45–66.
- Morishita, T., Dilek, Y., Shallo, M., Tamura, A., Arai, S., 2011. Insight into the uppermost mantle section of a maturing arc: the Eastern Mirdita ophiolite, Albania. *Lithos* 124, 215–226.
- Najafzadeh, A.R., Arvin, M., Ahmadipour, H., 2008. Podiform Chromitites in the Sorkhband Ultramafic complex, Southern Iran: evidence for Ophiolitic Chromitite. *J. Sci. Islam. Repub. Iran* 19, 49–65.
- Nimis, P., Taylor, W.R., 2000. Single clinopyroxene thermobarometry for garnet peridotites. Part I. Calibration and testing of a Cr-in-Cpx barometer and an enstatite-in-Cpx thermometer. *Contrib. Mineral. Petrol.* 139, 541–554.
- Niu, Y., 2004. Bulk-rock Major and Trace Element Compositions of Abyssal Peridotites: Implications for Mantle Melting, Melt Extraction and Post-melting Processes beneath Mid-Ocean Ridges. *J. Petrol.* 45, 2423–2458.
- Niu, Y., Langmuir, C.H., Kinzler, R.J., 1997. The origin of abyssal peridotites: a new perspective. *Earth Planet. Sci. Lett.* 152, 251–265.
- Pagé, P., Bédard, J.H., Schroetter, J.M., Tremblay, A., 2008. Mantle petrology and mineralogy of the Thetford Mines Ophiolite complex. *Lithos* 100, 255–292.
- Palme, H., O'Neill, H.S.C., 2003. Cosmochemical estimates of mantle composition BT - treatise on geochemistry. *Treatise Geochem.* 2, 1–38.
- Parkinson, I.J., Pearce, J.A., 1998. Peridotites from the Izu-Bonin-Mariana forearc (ODP Leg 125): evidence for mantle melting and melt-mantle interaction in a supra-subduction zone setting. *J. Petrol.* 39, 1577–1618.
- Pearce, J.A., Barker, P.F., Edwards, S.J., Parkinson, I.J., Leat, P.T., 2000. Geochemistry and tectonic significance of peridotites from the South Sandwich arc-basin system, South Atlantic. *Contrib. Mineral. Petrol.* 139, 36–53.
- Potts, P.J., Kane, J.S., 2007. International Association of Geoanalysts Certificate of Analysis: Certified Reference Material OU-6 (Penrhyn Slate). *Geostand. Geoanalytical Res.* 29, 233–236.
- Qi, L., Jing, H., Gregoire, D.C., 2000. Determination of trace elements in granites by inductively coupled plasma mass spectrometry. *Talanta* 51, 507–513.
- Ringuette, L., Martignole, J., Windley, B.F., 1999. Magmatic crystallization, isobaric cooling, and decompression of the garnet-bearing assemblages of the Jijal sequence (Kohistan terrane, western Himalayas). *Geology* 27, 139–142.
- Rollinson, H., Adetunji, J., 2013. Mantle podiform chromitites do not form beneath mid-ocean ridges: a case study from the Moho transition zone of the Oman ophiolite. *Lithos* 177, 314–327.
- Saccani, E., Dilek, Y., Photiades, A., 2017. Time-progressive mantle-melt evolution and magma production in a Tethyan marginal sea: a case study of the Albanide-Hellenide ophiolites. *Lithosphere* 10, 35–53.
- Saka, S., Uysal, I., Akmaz, R.M., Kaliwoda, M., Hochleitner, R., 2014. The effects of partial melting, melt-mantle interaction and fractionation on ophiolite generation: Constraints from the late cretaceous Pozanti-Karsanti ophiolite, southern Turkey. *Lithos* 202, 300–316.
- Schaltegger, U., Zeilinger, G., Frank, M., Burg, J.P., 2002. Multiple mantle sources during island arc magmatism: U-Pb and Hf isotopic evidence from the Kohistan arc complex, Pakistan. *Terra Nova* 14, 461–468.
- Snow, J.E., Dick, H.J.B., 1995. Pervasive magnesium loss by marine weathering of peridotite. *Geochim. Cosmochim. Acta* 59, 4219–4235.
- Sun, S., McDonough, W.F., 1989. Chemical and isotopic systematics of oceanic basalts: implications for mantle composition and processes. *Geol. Soc. London. Spec. Publ.* 42, 313–345.
- Taylor, W.R., 1998. An experimental test of some geothermometer and geobarometer formulations for upper mantle peridotites with application to the thermobarometry of fertile lherzolite and garnet websterite. *N. Jb. Miner. Abh.* 172, 381–408.

- Thompson, M., Potts, P.J., Kane, J.S., Webb, P.C., Watson, J.S., 2000. GeoPT4. An international proficiency test for analytical geochemistry laboratories - report on Round 4 (March 1999). *Geostand. Geoanalytical Res.* 24, 1–37.
- Uysal, I., Tarkian, M., Sadiklar, M.B., Zaccarini, F., Meisel, T., Garuti, G., Heidrich, S., 2009. Petrology of Al- and Cr-rich ophiolitic chromitites from the Muğla, SW Turkey: Implications from composition of chromite, solid inclusions of platinum-group mineral, silicate, and base-metal mineral, and Os-isotope geochemistry. *Contrib. Miner. Petrol.* 158, 659–674.
- Van der Laan, S.R., Flower, M.F.J., Koster von Groos, A.F., 1989. Experimental evidence for the origin of boninites: near liquidus phase relation to 7.5 kbar. *Boninites Relat. Rocks* 112–147.
- Wilson, M., 1989. *Igneous Petrogenesis: A Global Tectonic Approach* pp. 466.
- Woodland, S.J., Pearson, D.G., Thirlwall, M.F., 2002. A platinum group element and Re-Os isotope investigation of siderophile element recycling in subduction zones: Comparison of Grenada, Lesser Antilles Arc, and the Izu-Bonin Arc. *J. Petrol.* 43, 171–198.
- Wu, W., Yang, J., Dilek, Y., Milushi, L., Lian, D., 2017. Multiple episodes of melting, depletion, and enrichment of the Tethyan mantle: Petrogenesis of the peridotites and chromitites in the Jurassic Skenderbeu massif, Mirdita ophiolite, Albania. *Lithosphere* 10, 54–78.
- Xiong, F., Yang, J., Robinson, P.T., Xu, X., Liu, Z., Li, Y., Li, J., Chen, S., 2015. Origin of podiform chromitite, a new model based on the Luobusa ophiolite, Tibet. *Gondwana Res.* 27, 525–542.
- Xiong, F., Yang, J., Robinson, P.T., Dilek, Y., Milushi, L., Xiangzhen, X.U., Zhou, W., Zhang, Z., Rong, H., 2017. Diamonds Discovered from High-Cr Podiform Chromitites of Bulqiza, Eastern Mirdita Ophiolite, Albania. *Acta Geol. Sin.* 91, 455–468.
- Xiong, F., Dilek, Y., Wirth, R., Xu, X., Yang, J., 2019. Opx-Cpx exsolution textures in lherzolites of the Cretaceous Purang Ophiolite (S. Tibet, China), and the deep mantle origin of Neotethyan abyssal peridotites. *International Geology Review* 62, 665–682. <https://doi.org/10.1080/00206814.2019.1627678>.
- Xu, X., Yang, J., Ba, D., Guo, G., Robinson, P.T., Li, J., 2011. Petrogenesis of the Kangjinla peridotite in the Luobusa ophiolite, Southern Tibet. *J. Asian Earth Sci.* 42, 553–568.
- Yamamoto, H., Nakamura, E., 2000. Timing of magmatic and metamorphic events in the Jijal complex of the Kohistan arc deduced from Sm-Nd dating of mafic granulites. *Geol. Soc. London. Spec. Publ.* 170, 313–319.
- Yamamoto, H., Yoshino, T., 1998. Superposition of replacements in the mafic granulites of the Jijal complex of the Kohistan Arc, northern Pakistan: dehydration and rehydration within deep arc crust. *Lithos* 43, 219–234.
- Zhang, P.F., Uysal, I., Zhou, M.F., Su, B.X., Avci, E., 2016. Subduction initiation for the formation of high-Cr chromitites in the Kop ophiolite, NE Turkey. *Lithos* 260, 345–355.
- Zhou, M.F., Robinson, P.T., Malpas, J., Edwards, S.J., Qi, L., 2005. REE and PGE geochemical constraints on the formation of dunites in the Luobusa ophiolite, Southern Tibet. *J. Petrol.* 46, 615–639.
- Zhou, M.F., Robinson, P.T., Su, B.X., Gao, J.F., Li, J.W., Yang, J.S., Malpas, J., 2014. Compositions of chromite, associated minerals, and parental magmas of podiform chromite deposits: the role of slab contamination of asthenospheric melts in suprasubduction zone environments. *Gondw. Res.* 26, 262–283.